Int J Earth Sci (Geol Rundsch) (2007) 96:743–767
DOI 10.1007/s00531-006-0120-8

ORIGINAL PAPER

Three-dimensional sedimentary architecture of Quaternary sand and gravel resources: a case study of economic sedimentology (SW Germany)

Boris Kostic · M. Peter Süss · Thomas Aigner

Received: 12 December 2005 / Accepted: 6 July 2006 / Published online: 6 September 2006

Abstract Quaternary sands and gravels form important, yet often highly heterogeneous economic deposits. Detailed 3-D analysis of the sedimentary structure and stratigraphy of these deposits allows for an accurate estimation of exploitable material. This paper presents a case study in SW Germany reconstructing the 3-D distribution of glacial sediments based on a high-resolution, process-orientated sedimentary facies classification and lithostratigraphy integrated within the geo-modelling package gOcad. Situated along the maximal ice-extent of the Rhine glacier during the last glaciation, the study area is characterised by a morphologically prominent terminal moraine and its associated sandur, which form the stratigraphically youngest sediments of a glacial basin, partially exposed in two gravel pits. These outcrops helped to reconstruct the complex sedimentary architecture of the northern part of the glacial basin. The regional analysis is based on core data, as well as geoelectric and geomagnetic surveys. All data were integrated into km-scale, high-resolution geological 3-D models, depicting the large-scale dynamics of multiple glacier advances and retreats during the Early to Late Pleistocene. These models allow quantifying the thickness and volume distribution of exploitable sandy gravel and help to evaluate the occurrence of non-exploitable interbedded diamicton horizons. The high quality and quantity of gravels particularly north of the terminal moraine classifies the investigated area as very prospective for raw materials exploitation in the future.

Keywords Economic mineral resources · Gravel deposits · 3-D modelling · Quaternary · SW Germany

B. Kostic · M. P. Süss · T. Aigner (✉)
Institute of Geosciences, University of Tübingen,
Sigwartstrasse 10, 72076 Tubingen, Germany
e-mail: thomas.aigner@uni-tuebingen.de

Present Address:
B. Kostic
Badley Ashton & Associates Ltd., Winceby House,
Winceby, Horncastle LN9 6PB, UK

Introduction

Three-dimensional geological models integrating data from a variety of sources form an integral part in petroleum reservoir studies (e.g. Grammer et al. 2004). Similarly, 3-D sedimentary models become increasingly important in hydrogeological and aquifer characterisation studies (e.g. Bridge and Hyndman 2004; MacCormack et al. 2005). The present paper presents a case study of how the integration of sedimentological and geophysical data can be utilised to evaluate the 3-D architecture of sedimentary raw materials and their resource potential. We develop a hierarchic workflow starting with description of individual lithofacies types that compose depositional elements, common in glacial environments. The stacking of these depositional elements defines lithofacies associations, which in turn compose individual regional-scale geobodies. These geobodies represent major aquifer compartments and reflect the grain size distribution in production scale. They form the regional base to predict the spatial distribution, quality and potential of raw materials and aid to explore new production sites.

The field work for this study was carried out east of Ostrach in Upper Swabia (SW Germany, Fig. 1) as

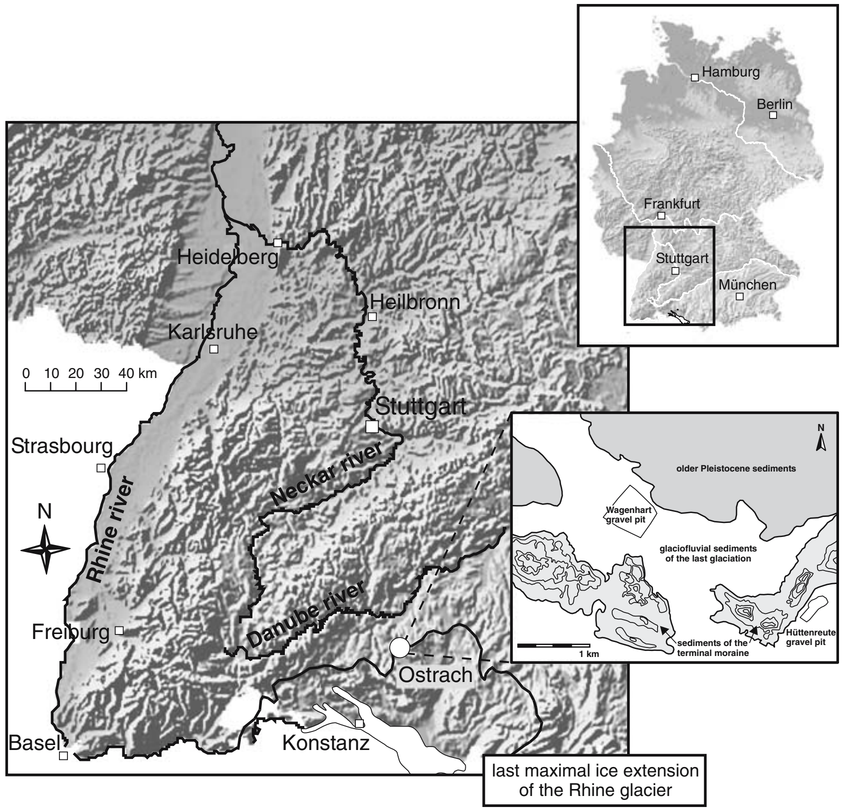

Fig. 1 The study area is located east of Ostrach (Upper Swabia, SW Germany) and exposes coarse-grained outwash and glacial diamicton deposits of the Würmian Rhine glacier in two gravel pits located to the north and south of the terminal moraine, respectively (see *inlet*)

part of the exploration and mapping program of the Landesamt für Geologie, Rohstoffe und Bergbau Baden-Württemberg (LGRB—Geological Survey of Baden-Württemberg) (Heinz 2002). The investigated deposits were formed during several climate cycles of the Middle and Late Pleistocene (Fig. 2) recording repeated northward-directed advances of the Rhine glacier into the Alpine foreland, progressively filling the Hosskirch Basin. The Hosskirch Basin represents a filled subglacial palaeovalley that was eroded into the Tertiary Molasse during the 'most extensive glaciation' (MEG) at the Early to Middle Pleistocene transition (Ellwanger et al. 1995). The 'last glacial maximum' (LGM), which represents the last maximum northern ice extent of the Rhine glacier in SW Germany, is documented in the study area by a terminal moraine that forms a prominent topographic ridge (Schreiner 1992).

Fluvial drainage of the Rhine glacier during this time occurred northward to the river Danube closely following older valley morphologies that were generated during previous glacial periods. The meltwater streams deposited coarse-grained outwash sediments, forming a sandur north of the terminal moraine. The sandur shows a clear transition to the terminal moraine and is characterised by steep gradients (about 11 m/km) in proximal and more gentle gradients (about 8 m/km) in distal zones, a few kilometres away from the former ice margin. The funnel shape of the sandur is caused by older Pleistocene deposits that occur in the north and northwest confining the development of a broad outwash plain (see inlet Fig. 1). A gravel pit on the sandur exposes the proglacial glaciofluvial sediments. A second investigated gravel pit is situated south of the terminal moraine and exposes glacial meltwater deposits interbedded with diamicton deposits that show features of glaciotectonic deformation.

The glaciofluvial sandy gravel deposits represent mineral resources of generally high quality. They are currently exploited in several gravel pits in the area. As the majority of the near-surface gravel deposits are located in the direct vicinity of the terminal moraine, they are commonly associated with interbedded, non-exploitable diamicton layers. Quantifying the spatial distribution of these deposits allows to predict their quality and volume and also to explore new exploitation sites.

Lithofacies

Lithofacies types are defined according to grain size distribution, texture, roundness of individual particles, sorting, fabric and stratification. In outcrop and in wells

Fig. 2 Climate/lithostratigraphic summary of the Quaternary in Baden-Württemberg (SW Germany); slightly modified after Villinger (2003)

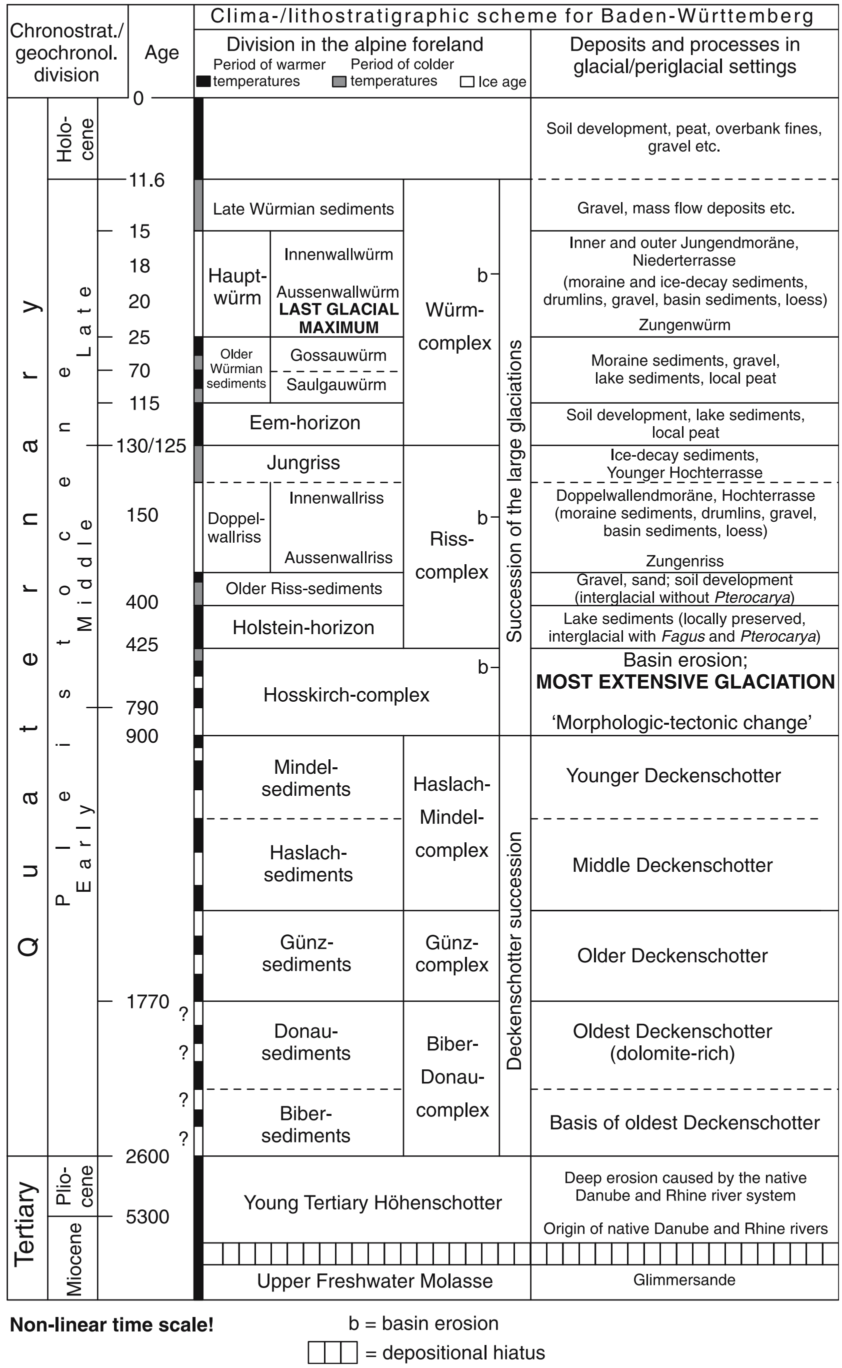

lithofacies codes were used in a purely descriptive sense for recording lithofacies properties. Our scheme is based on Keller (1996) and Heinz et al. (2003).

In this study the greater number of lithofacies types were formed by fluvial processes in a gravel-bed river. However, proximal to the terminal moraine gravitational processes affected the glaciofluvial depositional environment by remobilising glacial debris that was finally deposited within the coarse-grained meltwater sediments. The major lithofacies types that were recognised in the glaciofluvial deposits of the Rhine glacier are (Fig. 3): (1) cobble- and boulder-rich gravels (c,bGcm,i), (2) ill-sorted gravels [Gcm,(i); Gcx], (3) alternating gravels [(c)Gcg,a], (4) well-sorted gravels (GS-x), (5) stratified sands (S-x). Locally interbedded within these deposits are three lithofacies types that are distinguished by their diamictic composition: (6) matrix-supported diamictons (Dmm), (7) clast-supported diamictons (Dcm), and (8) sand-dominated heteroliths (sH-x) (Fig. 3). Here we present a short

litho-facies-code	photo	characteristic grain size distribution	description & interpretation
(1) cGcm,i - bGcm,i	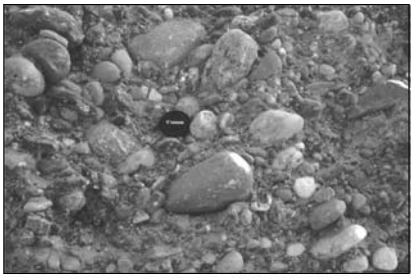	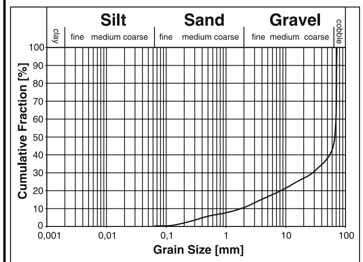	<u>cobble- & boulder-rich gravel</u> - clast-supported - well-rounded, infrequently subrounded to subangular components - poor to very poor sorting - imbrication of larger clasts: a(t), b(i) or a(p), a(i) - bed thickness: >40cm ***stream-driven, high-density traction carpets***
(2) Gcm,(i); Gcx	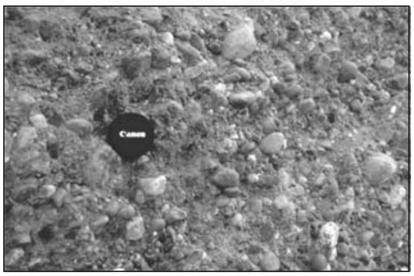	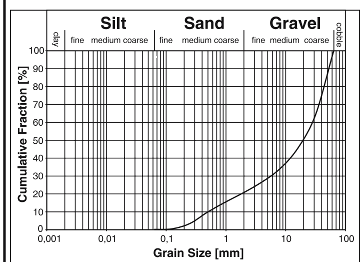	<u>ill-sorted gravel</u> - clast-supported - moderate to poor sorting - well- to rounded components - cross-stratified beds: a-axis parallel to bedding - horizontal beds: larger clasts are often imbricated a(t), b(i) - bed thickness: 10-30cm ***low-density tractional bedload sheets***
(3) (c)Gcg,a	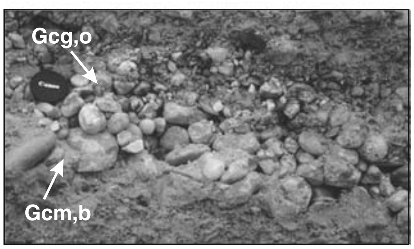	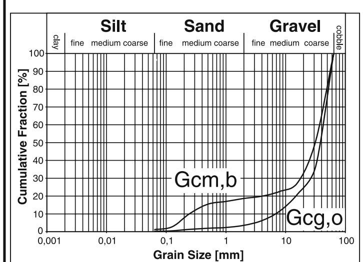	<u>alternating gravel</u> - clast-supported, graded - well-rounded components - upper zone: matrix-free (Gcg,o) - lower zone: bi- to polymodal (Gcm,b - Gcm) - bed thickness: 5-30cm ***low-density bedload sheets (deposited on inclined step)***
(4) GS-x	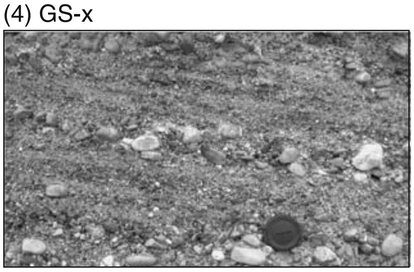	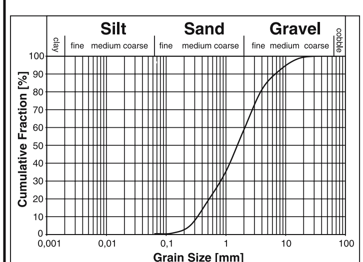	<u>well-sorted gravel</u> - clast-supported gravel to matrix-supported sand/ gravel mixtures - well-rounded components - well sorting - internal cross-stratification - bed thickness: 10-50cm ***tractional bedload transport***
(5) S-x	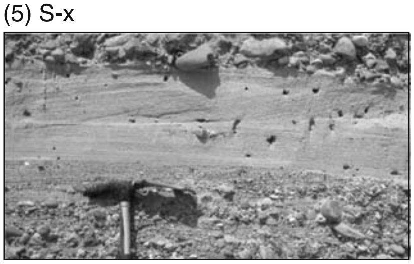	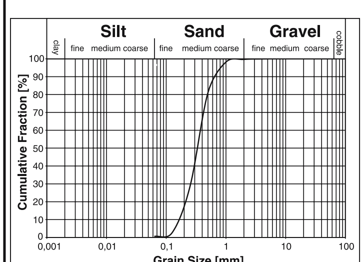	<u>stratified sand</u> - well sorting - forms horizontal and cross-stratified layers - bed thickness: 5-30cm ***bedload transport as single particles***

Fig. 3 Summary of the major lithofacies exposed in the Quaternary gravel pits in the Ostrach region

litho-facies-code / photo	characteristic grain size distribution	description & interpretation
(6) Dmm 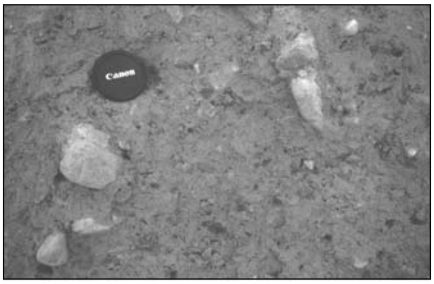	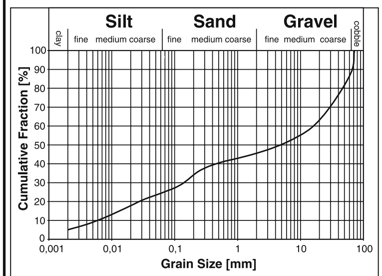	<u>matrix-supported diamicton</u> - matrix-supported - rounded to subangular components, partly striated - clast orientation may occur parallel to bedding a(p) or may show imbrication a(i) - erosive top with load casts - bed thickness: 10-250cm ***cohesive debris flow***
(7) Dcm 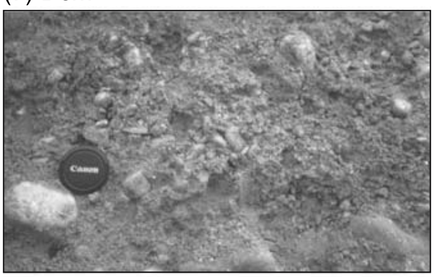	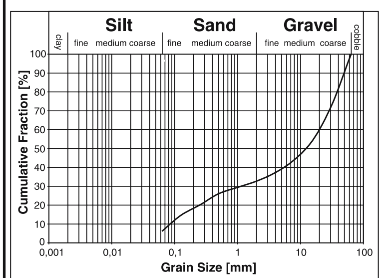	<u>clast-supported diamicton</u> - clast-supported - rounded to subrounded components - no preferred clast orientation - bed thickness: 10-200cm ***debris flow (higher degree of pore water)***
(8) sH-x 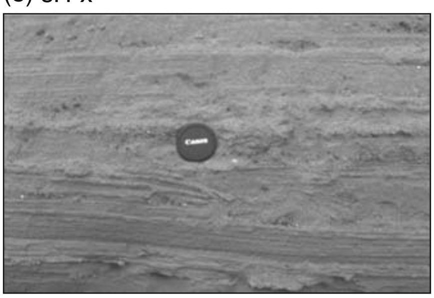	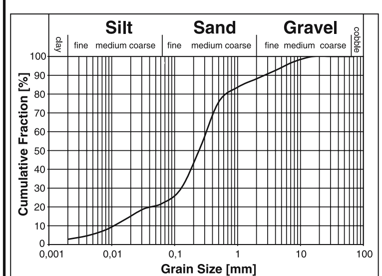	<u>sand-dominated heterolith</u> - alteration of sand- and fine-dominated (cm-thick) layers - infrequent intercalation of pebbles - total thickness: 10-50cm ***hyperconcentrated flow (rapid flow pulses)***

Fig. 3 continued

description of these lithofacies types and their generating processes.

1. Massive cobble- and boulder-rich gravels Massive cobble- and boulder-rich gravels commonly show imbrication of the larger clasts (*a*-axis transverse or parallel [*a*(t)/*a*(p)] to flow direction with either the *b*- or *a*-axis imbricated [*b*(i)/*a*(i)]). They are interpreted as the product of stream-driven, high-density traction carpets that account for a simultaneous en masse transport of the sand to boulder mixture (Todd 1989). This kind of transport requires high-magnitude suspension-rich floods.

2. Ill-sorted gravels Ill-sorted gravels are the most common lithofacies in the glaciofluvial deposits. They record deposition of low-density tractional bedload sheets (Steel and Thompson 1983; Smith 1990; Siegenthaler and Huggenberger 1993). Lack of sorting within the ill-sorted gravels implies rapid deposition during waning flows.

3. Alternating gravels Alternating gravels (composed of a lower zone of bi- to polymodal gravel and an upper zone of well-sorted openwork gravel) have often been described in the literature (e.g. Steel and Thompson 1983; Carling and Glaister 1987; Carling 1990; Siegenthaler and Huggenberger 1993). Different mechanisms are held responsible for their formation. While Steel and Thompson (1983) explained this alternation with flow fluctuations and clast segregation over the surface of a bar, Carling and Glaister (1987) experimentally produced horizontal alternating beds downstream of a negative step. Migration of gravel dunes across an oblique plane is suggested to form inclined alterations of this lithofacies (Siegenthaler and Huggenberger 1993).

4. Well-sorted gravels and 5. stratified sands Well-sorted gravels and stratified sands are locally interbedded with each other, but they are less common in the coarse-grained river deposits of the study area. Both lithofacies types document bedload transport of more or less single particles under low-energy flow conditions. Preservation of these lithofacies types is often restricted to local depressions where they form cross-stratified units and give way laterally to coarser sediments. Horizontal beds with horizontal and occasional cross-stratification also occur.

6. Matrix-supported diamictons Matrix-supported diamictons are interpreted as the product of cohesive debris flows which showed a high rate of shear during transport as indicated by a preferred clast orientation parallel to bedding a(p) or may show imbrication a(i) (Nemec and Steel 1984).

7. Clast-supported diamictons Clast-supported diamictons are less common compared to matrix-supported diamictons. The former lithofacies is characterised by a small clay/silt content (<10%), a high gravel fraction and a disorganised fabric. It is assumed that the clast-supported diamictons result from more water-rich debris flows with an increasing frictional component (Lawson 1988). The higher clast content together with a higher degree of sorting and clast roundness of this lithofacies relative to the matrix-supported diamicton has been argued by Levson and Rutter (1988) to indicate a greater degree of reworking by water and gravity prior to final deposition. However, an origin from heavily sediment-laden stream flows cannot be completely ruled out.

8. Sand-dominated heteroliths Sand-dominated heteroliths form lenses interbedded in gravel lithofacies. Thin alternations of fine- and sand-dominated layers indicate the deposition from hyperconcentrated flows. Rapid flow pulses may account for the rhythmical organisation of the deposit.

Depositional elements

Different types of gravel and diamicton depositional elements were identified on the basis of their external and internal geometries, as well as the nature of their bounding surfaces (Fig. 4). Within the gravel deposits two distinct groups of depositional elements were recognised: (1) cut-and-fill elements, which have an erosive, concave-up lower surface (e.g. hollows) subsequently filled with sediment (Fig. 5), and (2) accretionary elements which are characterised by a flat lower surface growing in a sheet-like aggradational style (Heinz et al. 2003; Fig. 6). They represent in-channel features, which were formed within the active river.

Cut-and-fill elements

Within the study area cut-and-fill elements vary mainly in their size. A distinction is made between long and deep features (ca. 5–15 m long, 0.5–2 m deep) and short and shallow features (ca. 1–5 m long, 0.2–0.4 m deep) that are interpreted to represent scour pool and dissection elements, respectively. They commonly show an asymmetric shape in flow-parallel sections, but tend to be more symmetrical in sections normal to palaeoflow.

Scour pool elements

Description The long and deep shapes of cut-and-fill elements are characterised by an erosive, concave-up lower bounding surface and a usually roughly horizontal upper surface (Fig. 5a). An erosive upper contact was commonly observed where these elements interfinger with each other vertically. The internal structure consists of trough cross-bedded sets of ill-sorted (Gcm, Gcx) and alternating gravel (Gcg,a) with only minor occurrence of well-sorted gravel (GS-x) and stratified sand (S-x).

Interpretation These elements are interpreted to represent scour pool fills formed at channel confluences or channel bends (Ashmore 1982). They represent scour hollows within the channel and are common in braided rivers (Best 1988; Best and Ashworth 1997). The geometry and infill of the ‘spoon-shaped’ scours observed in this study are similar to the migrating confluence scours described by Siegenthaler and Huggenberger (1993). In particular, the intimate interfingering of texturally different lithofacies types, indicating different bedload sources, renders an interpretation of these elements as scour pool fills plausible.

Dissection elements

Description The short and shallow forms of cut-and-fill elements show similar types of lower and upper

depositional element		extension [m] lateral	extension [m] vertical	lithofacies	sedimentation process
diamicton elements	massive lobes	>100	0.5-2.5	Dmm, Dcm, sH-x	sediment gravity flows
	thin layers	5-50	0.1-0.5		
ACCRETIONARY ELEMENTS					
horizontally-bedded gravel elements		20-50	0.2-0.4	Gcm,(i)	vertical and lateral accretion of gravel sheets
massive gravel elements		20-80	0.4-2	c,bGcm,i	accumulation of high-density traction carpets
stratified sand elements	horizontal stratification	2-20	0.05-0.3	S-x	vertical accretion of sandy bedload layers
	cross-stratification				progradation by foreset deposition
CUT-AND-FILL ELEMENTS					
scour pool elements	trough cross-stratification	5-15	0.5-2	Gcm, Gcx Gcg,a GS-x, S-x	trough fill by foreset deposition & lateral accretion
dissection elements	cross-stratification	1-5	0.2-0.4	GS-x, S-x (Gcm, Gcg,a)	shallow scour fill by foreset deposition

Fig. 4 The main depositional elements and associated lithofacies forming the gravel-bed braided-river deposits of the study area. Based on geometries and bounding surfaces two major forms of gravel depositional elements are identified: accretionary and cut-and-fill elements. Their quantified geometries in the present study correspond well with data collected by Heinz and Aigner (2003) within the northern palaeo-discharge zones of the Rhine glacier

bounding surfaces as those described for the scour pool elements. They mostly appear as isolated elements above horizontally bedded gravel sheets (Fig. 5b). Internally, cross-stratified sets of well-sorted gravel (GS-x) and stratified sand (S-x) dominate over ill-sorted (Gcm) and alternating gravel (Gcg,a).

Interpretation These shallow features are interpreted as small dissection elements of gravel bars. Flow across bar surfaces locally dissects the underlying bar units forming shallow scours (Bluck 1979). During falling stages they are likely to be infilled by lithofacies types typical for lower flow conditions before they are finally abandoned at low stage (Bluck 1974). Preservation of these high topographic positions within a gravel-bed river requires high aggradational rates of the depositional system (Bristow et al. 1993; Bristow 1996).

Accretionary elements

Accretionary elements occur as horizontally to sub-horizontally bounded depositional units that are 0.2–0.4 m thick or as massive units between 0.4 and 2 m in thickness. They are usually dominated by gravel lithofacies, but also 0.05–0.30 m thick sand-dominated elements were observed. The lateral extent is in the order of several tens of metres (about 20–80 m) for the gravel elements and several metres (about 5–20 m) for the sand elements. Generally, thicker elements tend to be more extensive.

Horizontally bedded gravel elements

Description The thinner accretionary gravel elements are very common in the study area and show flat lower and upper bounding surfaces (Fig. 6a). The lateral terminations appear to be gradual, commonly pinching out. A crude horizontal stratification results from the stacking of ill-sorted gravel beds (Gcm,(i)). The boundaries of individual beds are often vague but may be inferred from vertical textural variations comprising changes in maximum grain size, matrix content as well as clast orientation and from thin, intermittent sand layers. In few places, low-angle cross-strata were recognised adjacent to horizontal gravel sheets indicating an oblique cut relative to flow direction.

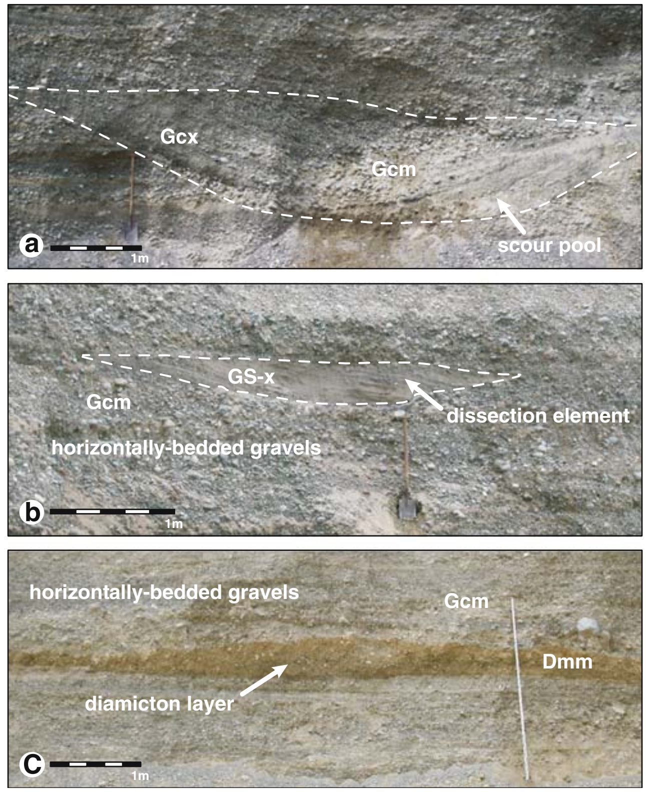

Fig. 5 **a** Cut-and-fill elements occur as long and deep forms containing gravel-dominated lithofacies and are interpreted to represent scour pool deposits. **b** Short and shallow forms of cut-and-fill structures comprising sand and gravel lithofacies are interpreted as small dissection elements of gravel bars. **c** Diamicton deposits form broad lobes and small layers of varying thickness interbedded within gravel deposits. In the studied outcrops they are exposed close to the terminal moraine and are interpreted to be the product of sediment gravity flows

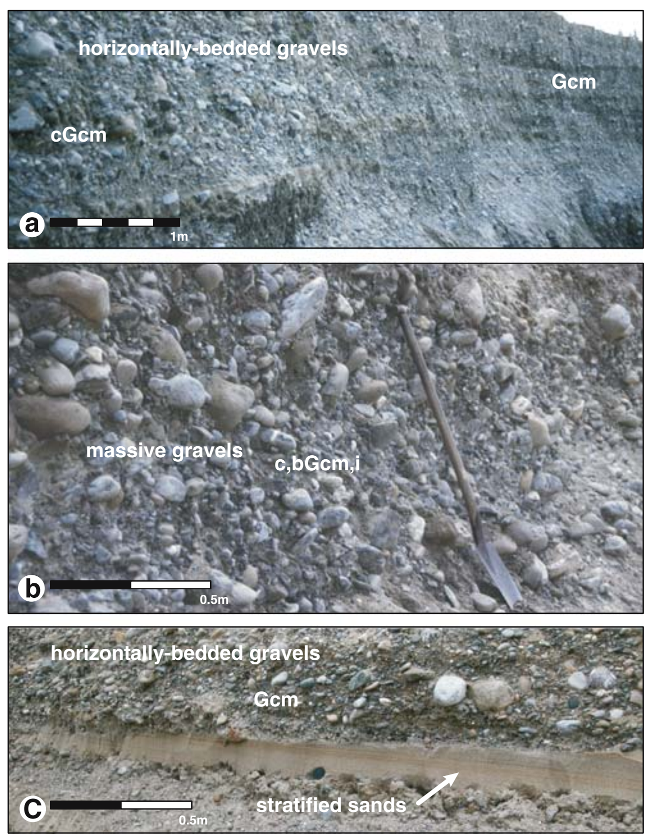

Fig. 6 **a** The most common type of depositional elements in the study area are horizontally-bedded gravel sheets. They form centimetre-thick units of commonly several tens of metres lateral extent indicative of gravel bars. **b** Massive, cobble- to boulder-rich gravel units are less common representing deposition from high-magnitude floods. **c** Cross-stratified sand units are rarely preserved within the gravel deposits and are interpreted to be the result of migrating sand bedforms under low-energy flow conditions

Interpretation The horizontally bedded gravel elements are interpreted as barforms. The nature of the ill-sorted gravel lithofacies indicates that these barforms were produced by the stacking of several pulsatory, low-density bedload sheets (Hein and Walker 1977). The internal structure and the dimensions (0.2–0.4 m thick, 20–50 m long) of the horizontally bedded gravel elements are similar to the longitudinal bars described by Boothroyd and Ashley (1975) for the upper reaches of two Alaskan outwash fans. These low-relief longitudinal bars show a general lack of foreset structures, which is compatible with own observations. This fact largely precludes a transverse bar origin for the horizontally bedded gravel elements as transverse bars are characterised by well-defined slipfaces at their downstream margin (e.g. Hein and Walker 1977). There is no clear evidence of bank attachments of the barforms or the presence of well-developed chute channels that would suggest the existence of lateral bars (Smith 1974; Bluck 1979).

Low-angle cross-beds that laterally pass into horizontal beds of ill-sorted gravel are interpreted as lateral accretion deposits (Ramos and Sopena 1983). Lateral modifications of longitudinal bars occur during falling stage, when flow direction is dispersed and diverges away from the bar-parallel orientation (Bluck 1974; Rust 1978).

Vertical textural variations observed within the gravel deposits are caused by flow fluctuations. Deposition of discrete sand layers within otherwise coarse-grained deposits occurs at falling and low stages (Boothroyd and Ashley 1975; Bluck 1979). In many cases the sand layers probably resemble relicts of stratified sand elements.

Massive gravel elements

Description The thick accretionary gravel elements are less common in the study area and are characterised by a massive appearance (Fig. 6b). They are composed entirely of cobble- and boulder-rich gravel (c,bGcm,i) with flat lower and upper bounding surfaces. Basal surfaces tend to be erosive. The massive gravel elements form massive single beds or sets of beds typically with relative abrupt lateral terminations.

Interpretation The massive appearance and simple geometry of these elements as well as their coarse clast size suggest a deposition from high-magnitude floods (cf. Marren 2001). These high-magnitude events generally have the potential to destroy and reorganise the whole fluvial system. Deposition occurred rapidly as indicated by the very poor sorting. There is little evidence for flow stage variations, falling-stage erosion, and reworking that is often associated with individual barforms.

Stratified sand elements

Description Thin sand elements are locally preserved within the gravel deposits and are more common in finer-grained gravel sections. They have flat bases or are moulded over the underlying coarser-grained beds (Fig. 6c). Their upper bounding surface is always erosive. Laterally, individual elements generally pinch out or are eroded and tend to end relatively abruptly. These elements are dominated by sand lithofacies (S-x) that is horizontally stratified or cross-bedded.

Interpretation Horizontally stratified sand elements are interpreted as upper-stage plane bed deposits, while cross-bedded elements are interpreted to be the result of migrating sandy bedforms (Harms et al. 1982). Their preservation potential within a gravel-bed river is relatively low.

Diamicton elements

Description Diamicton elements are interbedded within gravel deposits and predominantly occur in close proximity to the terminal moraine. They commonly form broad lobes but also occur as smaller layers with planar bases and erosive tops (Fig. 5c). They either represent thick (0.5–2.5 m) and massive units of several hundred metres in lateral extent or occur as thin (0.1–0.5 m) units that typically pinch out laterally after several metres to a few tens of metres (Fig. 7). Thickness is highly variable at short distances and single layers may be disrupted in places. Individual units can exhibit load casts. The diamicton elements are mainly composed of matrix-supported diamicton (Dmm) that may be associated laterally and vertically with clast-supported diamicton (Dcm) and sand-dominated heterolith (sH-x).

Interpretation The proximity of these elements to the terminal moraine, their predominant lobate shape, and characteristic lithofacies composition indicate a deposition from gravity flows. The lithofacies composition suggests that the diamicton deposits were formed by sediment flows of varying density ranging from cohesive debris flows to hyperconcentrated flows (cf. Zielinski and van Loon 1996). Load casts on the top of these elements indictate soft sediment deformation

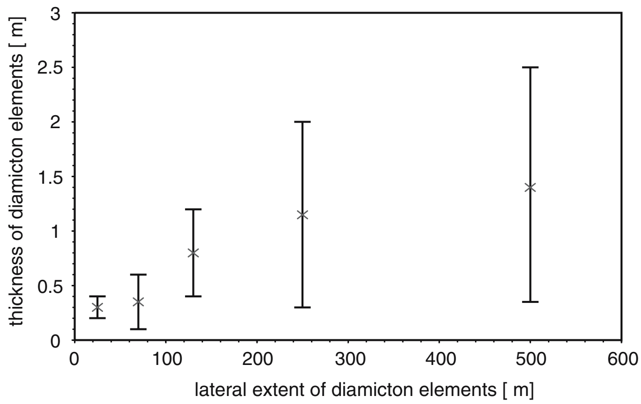

Fig. 7 Average thickness and thickness variations of diamicton elements in relation to their lateral extent. Thicker elements are generally more extensive, but show higher thickness variations that are largely due to postdepositional erosion of the soft sediments. This outcrop data served as an analogue in order to quantify the distribution of diamicton deposits in the subsurface within the 3-D models

while thickness variations are mainly attributed to postdepositional erosion by meltwater streams.

Stacking patterns and lithofacies associations in outcrops

The stacking pattern of depositional elements and associated lithofacies were studied in one active gravel pit located north (outer side) and one located south (inner side) of the terminal moraine. The analysis of the stacking patterns allows to define local-scale lithofacies associations (Table 1) and derived regional-scale geobodies that were used to quantify the raw material potential of the investigated area.

Wagenhart gravel pit: outer side of terminal moraine

Description This gravel pit exposes up to 15 m thick deposits of proglacial sediments that form a sandur in front of the terminal moraine. The sedimentary succession displays a vertical trend that is laterally consistent within the exposure (Fig. 8). The depositional architecture in the lower part of the section is dominated by horizontally bedded gravel elements that are locally intersected by small and shallow cut-and-fill elements. The latter are characterised by cross-bedded sets of well-sorted gravel (GS-x), stratified sand (S-x), and less commonly by alterations of poorly sorted (Gcm) and openwork gravel (Gcg,o). Genetically, they are interpreted to predominantly represent dissection

Table 1 The defined lithofacies associations consist of groups of successive, co-occurring lithofacies [lithofacies codes after Keller (1996) and Heinz et al. (2003)] and form the smallest units of the 3-D models

Code	Lithofacies association
F1	Fluvial association (S, gS, fS, sF)
GRS	Gravity-reworked-sediment association (D, Dm, Dc, sF, fS)
Gf	Glaciofluvial association (Gc, cGc, bGc, fGc, GS, S, gS, fS)
Gfw	Weathered glaciofluvial association (H, fS, D-,w)
Gl	Glaciolacustrine association (F, F-m, F-i, sF, fS, F-, d)
D	Diamicton association (D, Dm, sF)
Dw	Weathered diamicton association (H, D-,w)
Df	Mass flow diamicton association (D, Dm, Dc, sF)
Dt	Terminal diamicton association (D, cD, Dm, Dc, fGc)
Dd	Deformed diamicton association (D, Dm)

The association names were chosen either after the dominant lithology (e.g. diamicton association) or after the interpreted depositional environment (e.g. glaciofluvial association)

elements that modify the accretionary elements. The direction of cross bedding between different dissection elements may vary according to local flow patterns and largely depends on bar-channel geometry and discharge rate. Stratified sand elements are infrequently preserved within the gravel deposits.

The upper part of the section shows a marked increase in the average grain size. Long and deep scour pool elements occur more frequently and commonly interfinger with each other. Cross-beds mostly consist of ill-sorted (Gcm, Gcx) and alternating gravel (Gcg,o, Gcm,b). The direction of cross bedding in scour pools is less variable compared to smaller dissection elements and suggests an overall palaeotransport from the south/southeast. This trend was confirmed by the measurements of clast-imbrication within accretionary elements indicating a prevailing palaeocurrent direction from the southsoutheast. Gravelly accretionary elements dominate the uppermost part of the section and are only disrupted by relatively few sand-dominated dissection elements. A lobe-shaped diamicton element [dominated by matrix-supported diamicton (Dmm)] is interbedded within the succession of horizontally bedded [dominated by ill-sorted gravel (c)Gcm)] and occasionally massive gravel elements [mainly cobble-rich gravel (cGcm,i)]. The diamicton lobe is exposed across the entire outcrop and is

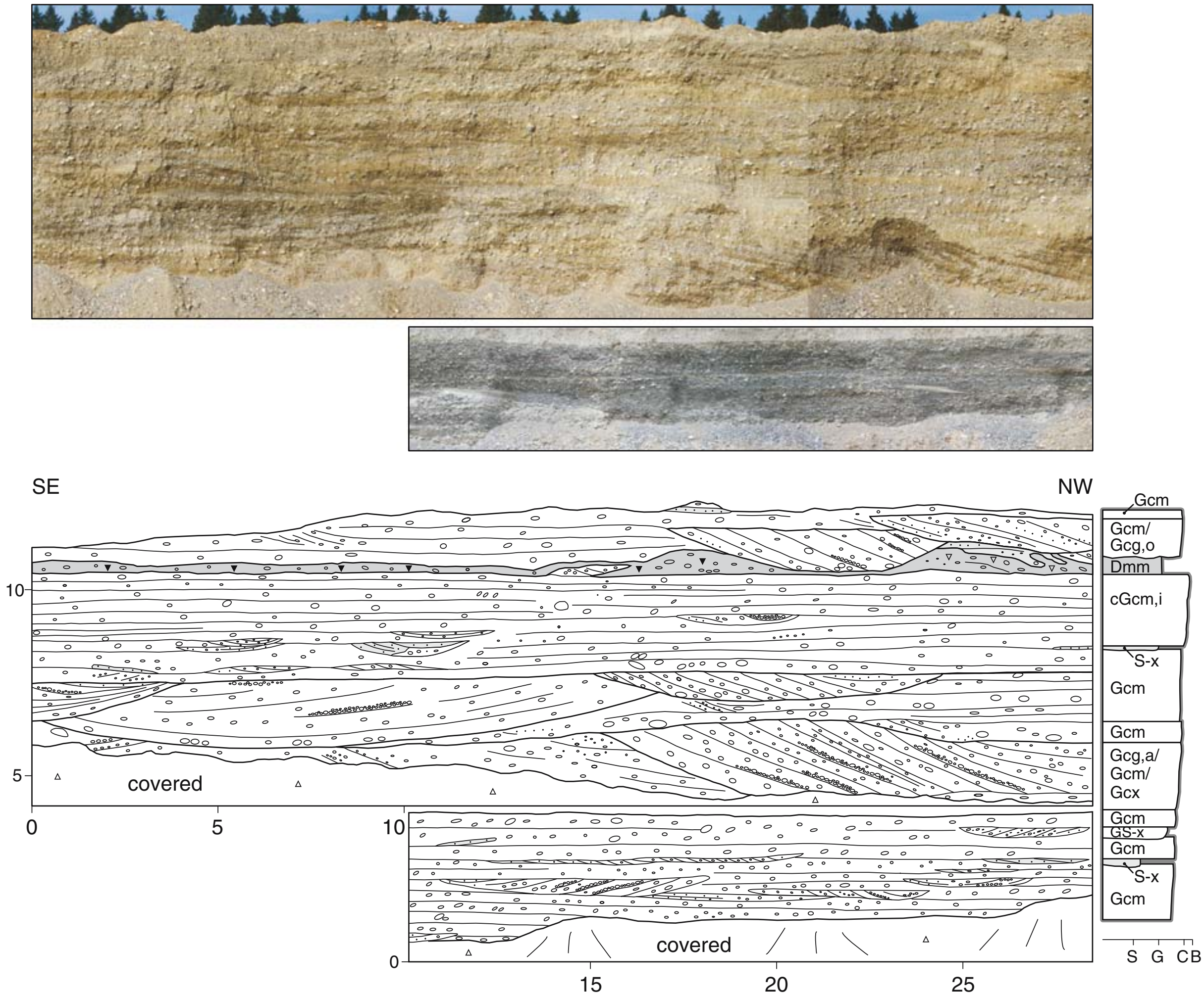

Fig. 8 The sedimentary architecture of the coarse-grained braided-river deposits exposed in the Wagenhart gravel pit is characterised by horizontally bedded gravel deposits that are intersected by small dissection elements and scour pools. The sequence illustrates a coarsening-upward trend that reflects increasing energy conditions indicating the advance of the Rhine glacier. Proximity to the glacier is documented by the interbedded diamiction lobe in the upper part of the succession

recovered in several sediment cores indicating a lateral extent of at least several hundred metres before finally pinching out. Local thickness variations of the diamicton deposit are the result of truncation by overlying scour pool elements and accretionary deposits. Generally, grain sizes of these upper gravel deposits are finer relative to the underlying gravel deposits.

Interpretation The proglacial deposits exposed in the Wagenhart gravel pit are dominated by horizontally bedded gravel elements with a low depth-to-width ratio. As outlined above, they are mainly considered to represent longitudinal bars. Together with massive gravel elements, scour pools, and small dissection elements, they form the fundamental depositional units characteristic for a braided-river system. The morphology of the sandur (steep proximal gradients) and the depositional setting in front of an ice mass provide favourable conditions for the establishment of a braided-river regime. The coarse grain sizes, poor sorting and internal structure of the bars imply high water discharge and relatively high sediment concentration in the flows. Sedimentation probably took place in relatively shallow channels as indicated by low-relief barforms and the absence of steeply inclined foreset strata. In order to develop significant cross-strata in gravel bars, considerable water-depth is required to produce an adequate bar-channel relief (Steel and Thompson 1983). The absence of fine-grained floodplain sediments suggests that the rates of channel migration were high enough to prevent the preservation of deposits at the highest palaeotopographic level. The dominance of bar deposits relative to pool fills suggests relatively high aggradation rates (Siegenthaler and Huggenberger

1993). High aggradation rates also account for the preservation of stratified sand elements and sand-dominated dissection elements that form mostly in the upper part of gravel bars.

The sedimentary succession of the Wagenhart section displays a coarsening-upward sequence. This is consistent with an upward decrease in sand facies and in sorting, and a general increase in the thickness and size of depositional elements. Massive gravel elements only occur in the upper section and their sparse and local distribution indicates low-frequency, high-magnitude flood events that have the potential to destroy and reorganise large parts of the fluvial system. This overall trend indicates increasing energy conditions and can best be explained by an advance of the Rhine glacier that finally terminated in the formation of a mass flow deposit (Heinz and Aigner 1999). Consequently, it reflects a shift from relatively distal to proximal reaches of the braided-river system. Most likely, deposition of the diamicton lobe is related to ice decay and glacier retreat following the maximum advance of the Rhine glacier. Glacier retreat is usually accompanied by high peak floods that most likely deposited the cobble-rich massive gravel elements underlying the diamicton deposits. The general decrease in grain size within the uppermost gravel deposits suggests a gradual decline in flow conditions and possibly documents the ongoing retreat of the ice mass.

In summary, the Wagenhart gravel pit is dominated by a glaciofluvial lithofacies association (Gf) and minor proportions of the diamicton facies association (D).

Hüttenreute gravel pit: inner side of terminal moraine

Description This gravel pit is located south of the terminal moraine and exposes 20 m thick glaciofluvial deposits along two sections. The northern outcrop wall is dominated by accretionary elements, while cut-and-fill structures are less common. The most characteristic features of this section are thick (dm-m) lenses of stratified sand-dominated heteroliths (sH-x) that extend for several metres to a few tens of metres in lateral direction. Here, this lithofacies typically occupies broad channel-like scours that are interbedded within ill-sorted and cobble- to boulder-rich gravel lithofacies. Matrix- and clast-supported diamicton elements are generally rare compared to the exposed southern section.

The southern outcrop wall can be subdivided into an undisturbed lower part and a glaciotectonically deformed upper part (Fig. 9). The undeformed lower part is similar to the lower succession of the northern exposure in terms of the geometry of depositional elements and the occurrence of lithofacies types. It predominantly consists of horizontally bedded gravel elements that are mainly composed of ill-sorted gravel (Gcm). Falling-stage sand (S-x) occurs as discontinuous lenses and less frequently as stratified sand elements on top of the gravelly accretionary elements. Cross-bedded stratified sand (S-x) and well-sorted sandy gravel (GS-x) fill small dissection elements that rarely contain cross-bedded gravels. Deep scour pool elements partly erode the lowermost exposed diamicton element, which can be traced across the gravel pit.

In the up-section there is an overall decrease in the occurrence of dissection elements and an absence of scour pool elements. Locally, massive gravel elements occur in the uppermost third of the exposure where they form laterally less extensive (<50 m) units. In some places, they contain reworked lenses of matrix-supported diamicton and boulder-sized clasts and define a general coarsening-upward trend within the vertical succession. As in the lower part, horizontally bedded gravel elements mainly consist of ill-sorted gravel [(c)Gcm]. They represent the dominant depositional element in the upper exposure, although here they are generally coarser and poorer sorted. Preservation of sandy falling-stage deposits is still common in the upper section. Interbedded diamicton elements become more common upwards and show evidence of glaciotectonic deformation. This mainly includes sheared diamictic bands associated with the tops of individual diamicton layers as well as up-thrusted segments of diamicton beds and outwash sediments. Deformation of diamicton layers is generally more pronounced in comparison to sand and gravel units. Only in areas characterised by high stress, gravel and sand layers are deformed and the clast-orientation of larger particles becomes gradually steeper. Imbrication measurements of clasts in the deformed and undeformed section, however, reveal no changes in palaeoflow direction and indicate a dominant flow from the east-southeast.

Interpretation The sedimentary succession in the Hüttenreute gravel pit implies deposition by glacial meltwater streams and sediment gravity flows in an ice-marginal setting. As in the Wagenhart gravel pit, the sedimentary architecture of the gravel deposits indicates the development of a low-sinuosity, most likely braided-river system that is characterised by a dominant accretionary sedimentation style. Principal differences between the two studied locations are

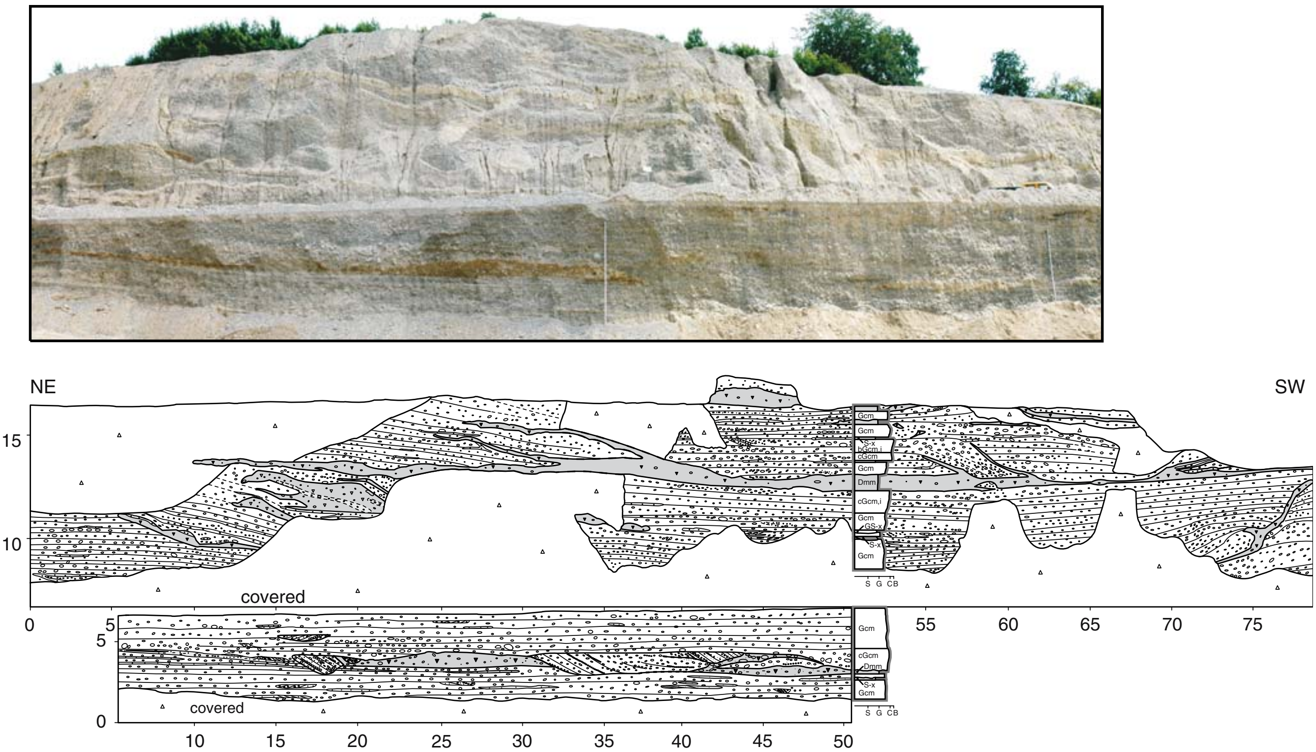

Fig. 9 Outcrop photo and field sketch of the south face of the Hüttenreute gravel pit. The sedimentary architecture is dominated by accretionary gravel elements and only minor cut-and-fill elements. Note the frequent interbedding of glacial diamicton deposits, which are particularly common in the glaciotectonically deformed upper half of the section (above ca.8 m). Upthrusting of sediment wedges is considered to be caused by small-scale fluctuations of the Rhine glacier following its maximal extent during the last glaciation

that the Hüttenreute exposures show fewer scour pool elements, a higher frequency of interbedded diamicton elements and modifications by glaciotectonics.

The rarity of scour pool structures suggests higher aggradation rates for the Hüttenreute location. The preservation of a relatively large number of falling-stage deposits and the local occurrence of massive depositional elements are evidences for some variability in the discharge pattern. The coarsening-upward character of the sequence is consistent with an overall decrease in sorting and reflects increasing energy conditions. This most likely results from a shift to proximal regions within the braided-river environment. Proximity to the ice-front, specifically for the upper part of the southern exposure, is indicated by several interbedded mass flow deposits.

The majority of the mass flow deposits are considered to be the product of debris flows and only few indicate deposition from hyperconcentrated flows. High-density mass flow deposits typically occur in the most proximal ice-marginal (terminoglacial) subenvironment (e.g. Zielinski and van Loon 1996) and are also common in proximal parts of the proglacial zone (e.g. Brodzikowski and van Loon 1987). Sedimentation in these subenvironments is largely determined by the vicinity of an ice mass and they are often subject to glaciotectonic deformation caused by an advancing glacier. Sediments of contrasting rheology, such as gravels, sands and diamictons react differently under the same stress field. Generally, diamictons exhibit lower resistance to stress (mainly due to high pore-water pressure) and are therefore potential zones of failure. Some of the diamicton elements have acted as basal failure planes causing the upward thrusting of semi-coherent sediment wedges in a northern direction. Within the Hüttenreute gravel pit glaciotectonic thrusting is restricted to the southern zone and glacially imposed stresses did not affect the northern part of the outcrop.

At present, the age of the glaciofluvial deposits in the Hüttenreute section relative to the Wagenhart location is unknown. It seems likely that they were formed during the course of small-scale oscillations of the Rhine glacier following its maximal advance that is associated with the formation of the sandur in the Wagenhart area. This hypothesis is favoured, as no evidence has been found that would suggest the overriding of the ice-marginal deposits by the advancing glacier (e.g. overconsolidation of sediments after entering the subglacial environment). However, an ice-marginal subglacial setting affected by relatively minor compressional pressure from the overlying ice cannot be totally excluded. Sediment deformation may have been caused by imposed lateral stresses pushing sediment wedges forward and slightly upward from their original position (Aber et al. 1989). Deposition of the Hüttenreute outwash sediments subsequently to the formation of the terminal moraine is furthermore suggested by palaeoflow data. Palaeoflow direction was dominantly from the east–southeast and hence occurred almost parallel to the course of the terminal moraine. The terminal moraine could have formed a topographic barrier that hindered northward-directed fluvial drainage of the Rhine glacier in this area causing meltwater streams to run along its southern margin.

Summarising, the Hüttenreute gravel pit consists of a massive base formed by a glaciofluvial facies association (Gf) and a subsequent succession of a deformed diamicton association (Dd).

3-D regional models of glacial deposits

In order to reconstruct the 3-D architecture of the glacial sediments on a kilometre-scale and to quantify the thickness and volume distribution of exploitable sandy gravel deposits, two 3-D regional models were generated using a database of more than 150 core descriptions, geoelectrical resistivity profiles and electromagnetic surveys (Fig. 10). The analysis of the exposed stratigraphic units and various cross sections integrating core and geophysical data provided the genetic framework for the 3-D reconstruction of the glacial deposits. The database offered a relatively dense measure of the spatial extent of the various deposits and locally allowed for their detailed 3-D mapping.

The core data and several geoelectrical resistivity profiles were derived from the database of the Landesamt für Geologie, Bergbau und Rohstoffe Baden-Württemberg (LGRB). Based on the original purpose of the drilling investigations (e.g. groundwater coverage, site investigations) the core descriptions varied in quality and therefore had to be evaluated before being used in this study. Additional drilling carried out on behalf of the LGRB during the time of

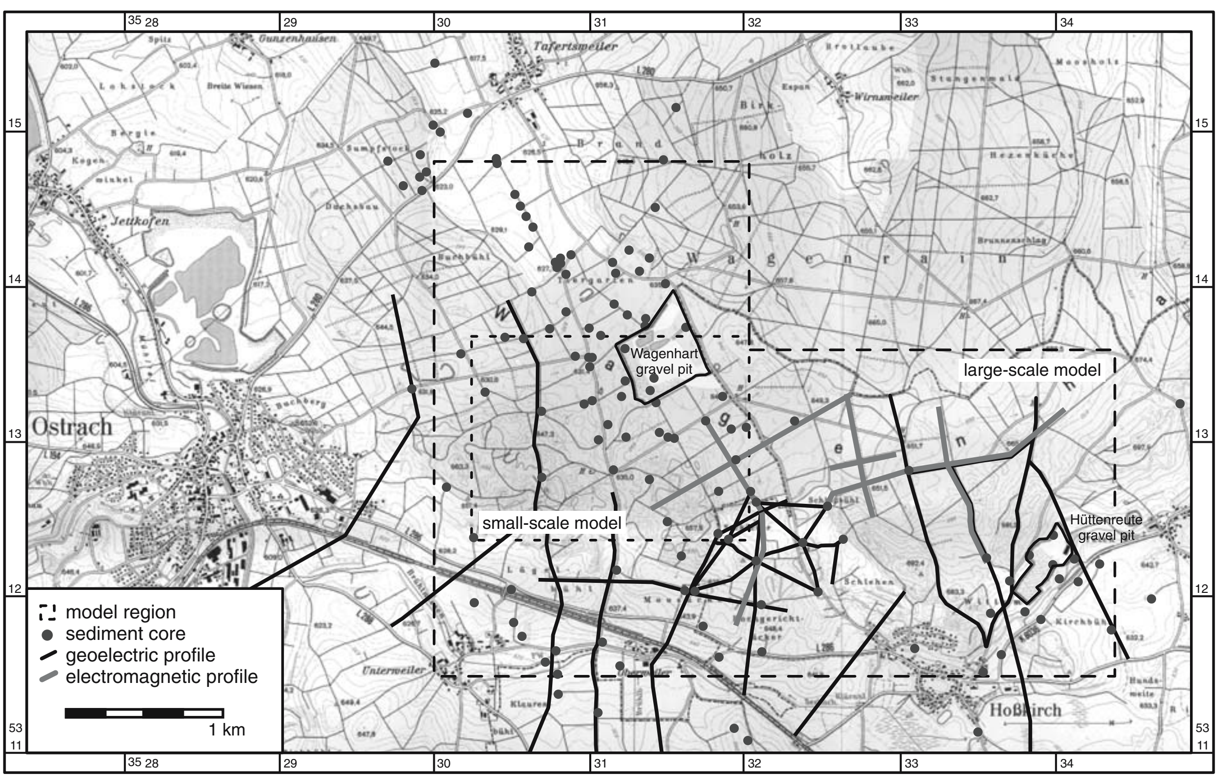

Fig. 10 The database of the study area in Upper Swabia consists of more than 150 sediment cores, multiple geophysical surveys and outcrop studies carried out in two gravel pits. Two regional 3-D models that differ in size and resolution are constructed by integrating the evaluated data

this study offered the opportunity to analyse recent core material. The core data were interpreted in terms of lithofacies using the standardised scheme applied in outcrop sedimentology.

Geoelectric resistivity and horizontal loop electromagnetic surveys were carried out in order to obtain additional subsurface information particularly in areas where core data were sparse. Data interpretation was constrained by comparison with existing core information. For a detailed overview of the applied geophysical methods see Becht (2004).

Model concept

Based on outcrop and core analysis lithofacies types were grouped to ten different lithofacies associations (Table 1). They represent the smallest units that can be modelled throughout the study area and account for the small-scale variations that are still resolvable on a basin-scale. Primary lithofacies types that were altered by postdepositional processes such as weathering were grouped into separate lithofacies associations representing their raw material properties. Weathering processes greatly affect the raw material quality of single components. Hence, depending on the degree and depth of weathering such deposits may only exhibit a minor raw material potential.

Lithofacies associations determine larger-scale 3-D geobodies that are typically several kilometres in lateral extent and several metres to a few tens of metres in thickness. Geobodies are characterised by the occurrence of either one or by a group of different, co-occurring lithofacies associations. They were defined on a lithological basis and therefore do not necessarily correspond to chronostratigraphic units. The seven geobodies (A–G) defined within the Quaternary sediments rest on Tertiary Upper Freshwater Molasse (southern part of models) and Upper Marine Molasse (northern part of models), respectively. To account for their raw material quality weathered and reworked surface deposits of Holocene and Late Pleistocene age were represented by a single geobody (geobody G). Because of their generally low raw material potential weathered surface deposits of Early and Middle Pleistocene age occurring in the north and northwest of the study area were not separated from their unweathered equivalent.

Model construction

Two regional 3-D geological models were developed for the northern Hosskirch Basin differing in size and resolution. Both models are represented by triangulated surfaces and regular orthogonal grids. A small-scale model with a horizontal grid size of 12 m × 9 m is embedded in a large-scale model possessing a horizontal grid size of 25 m × 25 m (see Fig. 10). The layer thickness for both grids is 0.5 m.

The generation of the 3-D models followed a two-step approach integrating all available sedimentological and geophysical data. The first step comprised the subdivision of the model into various geobodies by triangulated surfaces. In a second step, the spatial distribution of lithofacies associations was modelled within the gridded geobodies.

Definition of a layering scheme

Based on correlated 2-D cross sections (Fig. 11), various triangulated surfaces were mapped in gOcad confining distinct geobodies (Figs. 12, 13). These surfaces were constrained by core data and were locally adjusted to match geologic observations, such as data from the regional geologic map (Szenkler and Ellwanger 2001). Honouring the dense database and in order to minimise interpolation uncertainties, several surfaces were mapped within the prominent geobody E. These surfaces allowed to portray the inferred spatial distribution of individual lithofacies associations in detail.

The spatial distribution of the geobodies is constrained by the Quaternary unconformity and the present-day topography. The base of the Quaternary is steadily rising from the south (Hosskirch Basin) towards the north of the study area and exhibits a narrow incision in the northwest extending towards Tafertsweiler (Fig. 12). While the Quaternary unconformity was shaped to a large degree during the MEG (cf. Ellwanger et al. 2001), the present-day topography mostly reflects the distribution of the sediments deposited during the LGM. The most characteristic topographic feature associated with the LGM is the terminal moraine that forms a distinct west–east orientated ridge. Topographic highs in the north and northwest of the study area represent partly to mostly consolidated deposits from older glacial intervals (Early Pleistocene).

Geostatistical modelling of lithofacies associations

The spatial distribution of lithofacies associations was either determined through (1) detailed 3-D mapping honouring outcrop sedimentology (e.g. within geobody E; Figs. 12), (2) the distribution of a particular geobody in case one lithofacies association solely constituted a

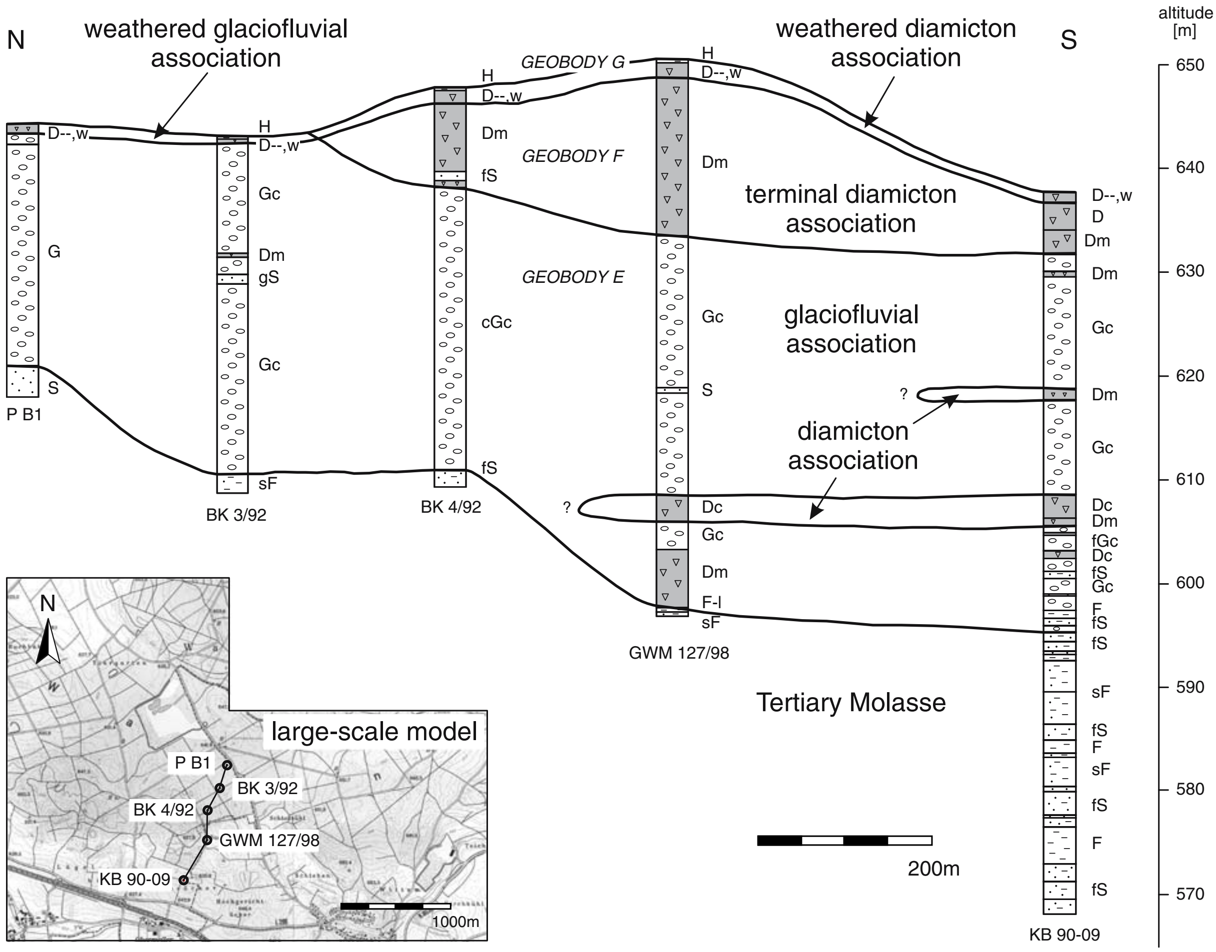

Fig. 11 Based on the lithofacies interpretation of core descriptions various 2-D cross-sections are constructed for the study area that indicate the lateral distribution of lithofacies associations and large-scale geobodies

single geobody (e.g. geobody B), or (3) geostatistical analysis of core descriptions.

Geostatistical analysis was used to guide the interpolation of the models and to determine the spatial relationships of individual lithofacies associations. The spatial trends of the interpreted and irregularly distributed core data were described through a variogram model (Table 2) by systematically calculating the average dissimilarities of parameters (here lithofacies associations) within a given class of distances and directions and fitting a theoretical spatial function (e.g. exponential) to the resulting experimental variogram (Deutsch and Journel 1992; Wackernagel 1998).

Based on the underlying variogram models, indicator kriging was applied to estimate the local distribution of lithofacies associations considering the distance and the spatial distribution of the sampled locations. Indicator kriging aims at minimising the variance of the estimation error and tries to determine the mean residual or error equal to zero (Isaaks and Srivastava 1989). It therefore provides the least risk model but has a tendency to underestimate the full range of parameter values.

Model results

Following the subglacial erosion of the Hosskirch Basin during the MEG, the complex succession of Quaternary sediments in the study area formed in response to several glaciations during Riss and Würm times. Although the sedimentary succession is generally dominated by glacial deposits, interglacial sediments of warmer climatic periods are locally preserved as well. They mainly comprise fine-grained sediments that indicate glaciolacustrine deposition (Ellwanger et al. 1995). The stratigraphic interpretation of the various deposits is still under discussion

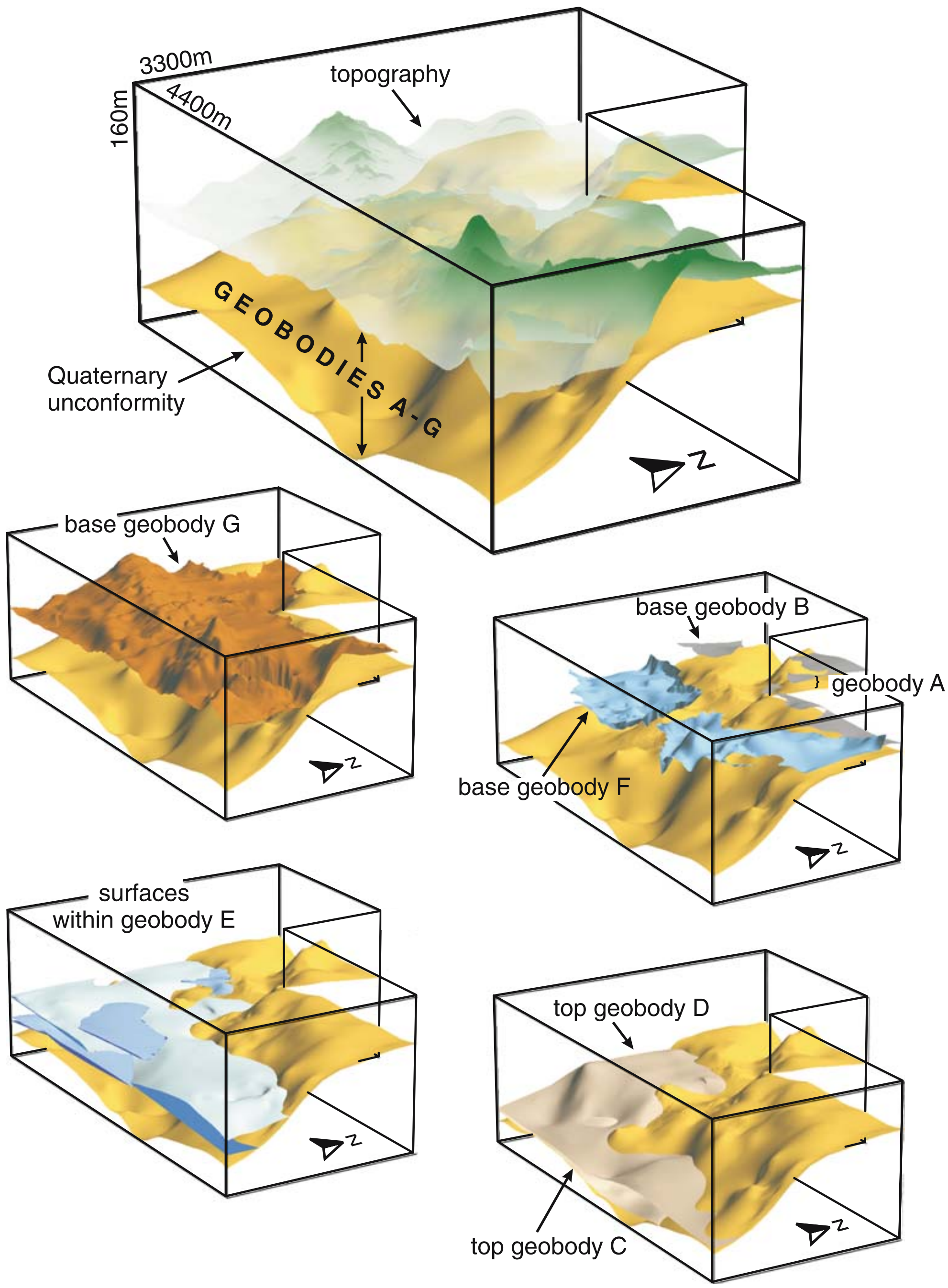

Fig. 12 Mapping of surfaces is used to derive the spatial distribution of geobodies. Within the enveloping Quaternary unconformity and the present-day topography of the large-scale model, seven geobodies (A–G) are defined in the study area. Various surfaces within geobody E allow the mapping of distinct lithofacies associations. Vertical exaggeration is 10

(e.g. Ellwanger et al. 1999, 2001, 2002; Villinger 2003) and this study is largely based on personal communication with D. Ellwanger (Table 3).

The Hosskirch Basin is transversely cut into a former valley of Early Pleistocene glaciofluvial sediments (younger Deckenschotter deposits). These deposits represent the oldest Quaternary accumulations in the area and define the northern margin of the large-scale model (Fig. 14). Southward, the large-scale model describes the course of the terminal moraine related to the LGM and stretches as far as the northern extension of the Hosskirch Basin. The small-scale model primarily portrays the distribution of sediments in the transition zone between the terminal moraine and the adjacent glaciofluvial sandur deposits east of Ostrach (Fig. 15).

Geobody A

Description Overlying the Tertiary Upper Marine Molasse geobody A defines the northern and northwestern termination of the large-scale model (see

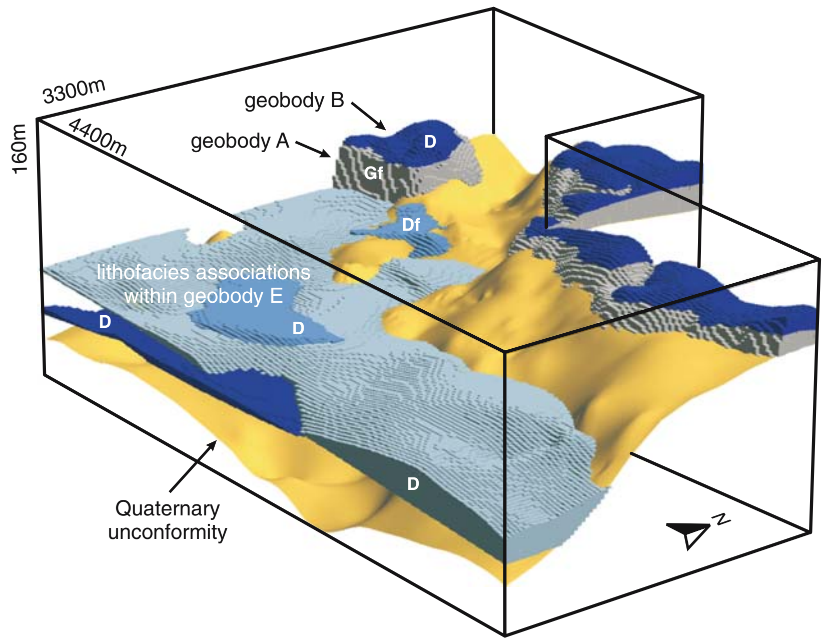

Fig. 13 Spatial distribution of mapped diamicton (D) and mass flow diamicton (Df) lithofacies associations within geobody E. The latter is exposed in the Wagenhart gravel pit and can be correlated between the outcrop and sediment cores, which were recovered in the vicinity of the gravel pit. Geobody A occurs in the north of the large-scale model and solely consists of glaciofluvial lithofacies associations (Gf) while geobody B is made up of diamicton lithofacies associations (D). Vertical exaggeration is 10

Table 2 Description and interpretation of geobodies that characterise the 3-D models of the study area

Geobodies	Description and interpretation
Geobody G	Weathered, gravity reworked and fluvial surface sediments (Gfw, Dw, GRS, Fl). Interpretation: Holocene and Late Pleistocene postglacial soil horizons, reworked surface deposits and fluvial sediments
Geobody F	Clast- and matrix-supported diamictons intercalated with diamictic sands, laminated fines and fine-rich gravels (Dt). Interpretation: terminal moraine deposits of the 'last glacial maximum'
Geobody E	Sand- and cobble-rich gravels interbedded with matrix- and clast-supported diamictons and diamictic sands or varying thickness and extent (Gf, D, Df), which are deformed in places (Dd). Fine-grained sediments are relatively rare (Gl). Interpretation: glaciofluvial and glacial moraine deposits associated with the Würm and Riss glaciations that are partly glaciotectonically deformed. Preservation of interglacial, glaciolacustrine fines
Geobody D	Laminated and massive fines and fine-rich sands that locally contain single gravel components (Gl). Interpretation: glaciolacustrine deposits largely related to the Holstein interglacial
Geobody C	Sandy diamictons intercalated with fine-rich gravels (D), coarse-grained basal lag. Interpretation: glacial moraine deposits mainly associated with the 'most extensive glaciation'
Geobody B	Matrix-supported, partly consolidated diamictons (D). Interpretation: glacial moraine deposits of the Doppelwallriss stage
Geobody A	Sand-rich, mostly consolidated gravels (Gf). Interpretation: Early Pleistocene gaciofluvial deposits

Fig. 13). It reaches a thickness of 5–10 m, but increases up to 25 m in the northernmost sections. Geobody A mainly consists of glaciofluvial sandy gravels (Gf) that are for the most part consolidated. They are commonly exposed in marginal areas above geobody E.

Interpretation Geobody A comprises the oldest Quaternary deposits of the study area associated with the Deckenschotter-succession (Early Pleistocene). They represent the southeastern occurrence of glaciofluvial deposits that form an extensive southwest to northeast trending belt north of the LGM terminal

Table 3 Computed variogram models that are used to quantify the local distribution of individual lithofacies associations within geobodies E and G of the large- and small-scale models

Model for	Lithofacies associations	Function	Azimuth	Dip	Sill	Range-*X*	Range-*Y*	Range-*Z*
Large-scale model								
Geobody E	Gf	Exponential	143.485	0.0	0.0844801	966.21	690.20	10.03
	Gl	Spherical	149.212	0.0	0.0764860	1,053.33	460.83	9.50
	D	Spherical	94.979	0.0	0.0700937	1,178.11	837.25	7.47
	Dd	Exponential	14.000	1.1	0.0277909	991.04	941.36	6.51
Geobody G	Fl	Spherical	126.461	0.0	0.0924404	730.79	286.04	2.12
	GRS	Exponential	80.603	0.0	0.0368821	496.06	175.46	3.52
	Gfw	Exponential	143.485	0.0	0.0771870	966.21	690.20	2.61
	Dw	Exponential	17.000	0.0	0.0137799	991.04	941.36	2.34
Small-scale model								
Geobody E	Gf	Exponential	127.134	0.0	0.0322841	854.63	646.93	6.00
	D	Exponential	105.098	0.0	0.0171119	1,076.95	720.72	7.29
Geobody G	GRS	Exponential	76.780	0.0	0.275398	456.28	140.01	2.78
	Gfw	Exponential	127.134	0.0	0.2150370	854.6	646.93	2.51

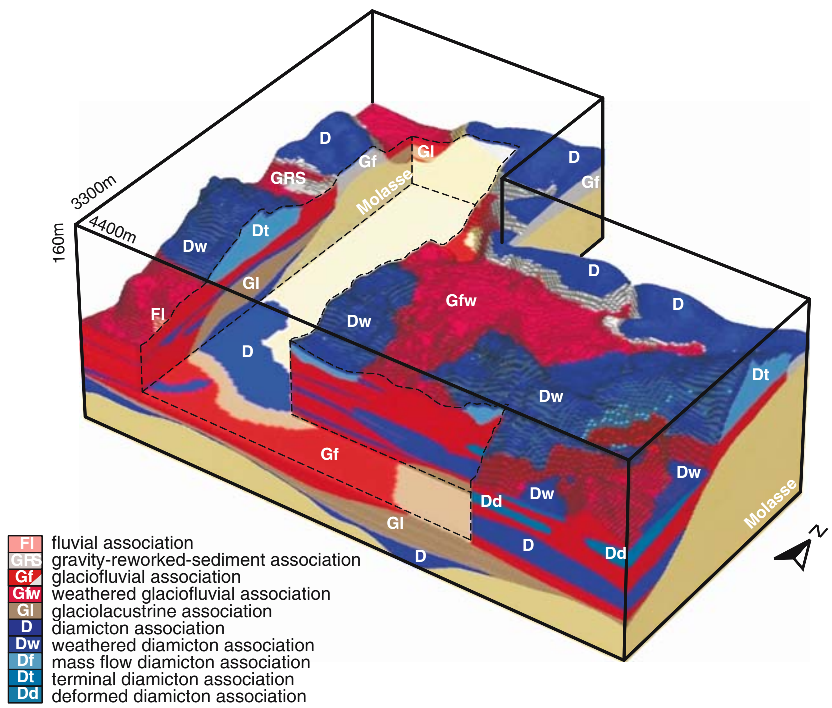

Fig. 14 Three-dimensional distribution of lithofacies associations within the large-scale model of the study area. Thick and widespread diamicton associations interbedded within glaciofluvial sediments occur in the Hosskirch Basin (southern part of the model). Note the steady rise of the Quaternary base towards the north and the glaciofluvial deposits of Early Pleistocene age in the northern part of the model (marked in *grey*). Weathered glaciofluvial and diamicton associations are only defined for Late Pleistocene sediments. Vertical exaggeration is 10

moraine. The younger Deckenschotter deposits were gradually eroded during subsequent glacial cycles and their recent distribution in the study region is particularly determined by the Jungriss erosion (Fig. 2) event in late Middle Pleistocene.

Geobody B

Description Covering geobody A, the distribution of geobody B is restricted to the north of the study area where it forms topographic highs. Its thickness typically increases in a northward direction and is in the range of several metres to 12 m at some locations. Matrix-supported, partly consolidated diamictons (D) predominate.

Interpretation Geobody B represents diamicton deposits that are linked to the Doppelwallriss stage. The deposits of geobody B extend farther north of the study region while time equivalent deposits in the northern Hosskirch Basin are locally preserved within geobody E.

Geobody C

Description Geobody C occurs in the south-western area of the large-scale model resting on Tertiary Upper

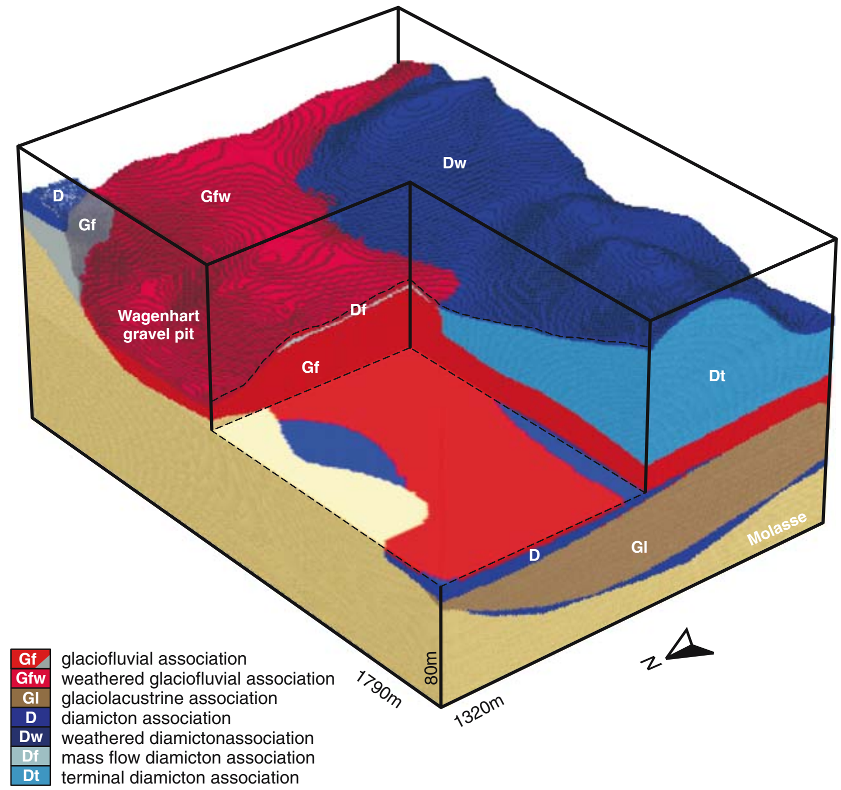

Fig. 15 Small-scale 3-D block model quantifying the distribution of lithofacies associations in the Wagenhart area. A prominent mass flow deposit (Df) is interbedded within the glaciofluvial association (Gf) of the sandur north of the terminal moraine (Dt). While these sediments are related to the last glacial maximum, the glaciofluvial association in the north-east corner of the model (marked in *grey*) represents parts of the Early Pleistocene Deckenschotter deposits. Vertical exaggeration is 10

Freshwater Molasse. Its northern extension is confined by Tertiary sediments. Geobody C partly levels off the Tertiary relief that resulted from subglacial erosion of the MEG. Thickness variations of several metres are typical and a maximum thickness of 17.5 m is reached at one location at the southern margin of geobody C. Geobody C is characterised by sandy diamictons with some fine-rich gravel interbeds (D). A cobble-rich basal lag was identified in some cores.

Interpretation Following the MEG erosion event, geobody C records the first accumulation episode in the Hosskirch Basin and adjacent northern areas. The coarse-grained basal lag and the occurrence of diamicton deposits at the base of the Hosskirch Basin suggest that these deposits are associated with the generation of the subglacial basin. They are interpreted to have formed in a depositional environment characterised by ice decay.

Geobody D

Description The occurrence of geobody D is generally limited to the south of the large-scale model but in the western part it extends far to the north directly overlying geobody C. The northern distribution of geobody D is terminated by Tertiary sediments. Thickness variations result in two thickness maxima up to 31 m in the south and west while in between the thickness is reduced to a few metres. In contrast to all other geobodies, geobody D is solely made up by laminated and massive fines and fine-rich sands (Gl). Individual layers locally contain single gravel components.

Interpretation The fine-grained sediments of geobody D are predominantly related to the Holstein interglacial. The thick and widespread deposition of laminated and massive fines implies a glaciolacustrine origin. The formation of a lake in the Hosskirch Basin was initiated during the course of glacier retreat and persisted long enough to allow the accumulation of thick fine-grained deposits. Thickness variations are most likely caused by subsequent erosion, which is indicated by the variable upper surface of geobody D.

Geobody E

Description Geobody E is the most prominent feature, which extends over large parts of the model area. It reaches a maximum thickness of 80 m in the southeast and with one exception at its western margin consistently decreases in thickness towards the north. Geobody E largely determines the present-day topography of the low-lying areas adjacent to the topographic highs comprised by geobodies B and F. Notably two extensions of geobody E stretch out westward and north-westward of the Wagenhart gravel pit erosively overlying Tertiary sediments. They are mainly composed of glaciofluvial gravels (Gf), but also comprise fine-grained deposits (Gl) that are particularly widespread in the northwest.

Geobody E shows a complex internal structure dominated by sand- and cobble-rich gravels (Gf) interbedded with diamictic sands and matrix- and clast-supported diamictons (D, Df) of varying thickness and lateral extension (see Fig. 7). Only some diamicton layers can be traced over distances of a few kilometres typically displaying thicknesses of 5–15 m. The most prominent and largely consolidated diamicton layer extends over the entire length of the model area and unconformably overlies the fine-grained deposits of geobody D in the west.

In the southeast, diamicton layers and associated gravel beds are often glaciotectonically deformed and locally form southward-dipping layers (Dd) that are partly exposed in the Hüttenreute gravel pit (see Fig. 8).

Interpretation The spatial distribution of lithofacies associations within geobody E is related to different glaciations during Riss and Würm times. Diamicton layers within the lower half of the succession are interpreted to be the product of different glacier advances during the Doppelwallriss and the Jungriss stages (cf. Ellwanger et al. 1995). These deposits are predominantly of subglacial origin as indicated for instance by the high degree of consolidation within the most prominent diamicton layer. In large parts of the model the top of this diamicton layer correlates with a distinct erosion event that formed the long incised valley towards Tafertsweiler. This erosion phase is most likely associated with a catastrophic postglacial ice decay caused by a climatic change at the end of the Jungriss stage (D. Ellwanger, personal communication). Coarse-grained meltwater deposits that are overlain by fine-grained sediments in the western, but particularly in the northwestern extensions of geobody E, record a period of warmer climate. The fine-grained sediments are interpreted to represent glaciolacustrine deposits that were formed in small depressions created through the erosion event.

The deposits within the uppermost part of the succession of geobody E formed in response to the LGM and record the development of a sandur north of the terminal moraine (geobody F). Diamictons and diamictic sands interbedded within these coarse-grained outwash sediments reflect mass flow deposits that indicate the local presence of an ice sheet. The course of the sediment-laden proglacial streams north of the glacier largely followed the older Jungriss depressions. In contrast to former glaciations, the LGM only had a minor erosional impact on the landscape in the study area. Instead of a pronounced erosion of Early and Middle Pleistocene as well as Tertiary sediments, this glacial period mainly reworked and accumulated thick deposits that shaped the present-day topography.

The deformation of diamicton and gravel layers in the southeast of geobody E most likely resulted from small-scale fluctuations of the glacier associated with the formation of the terminal moraine during the LGM (see above). Compression and deformation of ice-marginal sediments by the oscillating glacier was probably enforced by the nearby existence of the terminal moraine, which possibly functioned as a northern topographic barrier.

Geobody F

Description Geobody F forms two elongated flanking ridges that extend from the west to the east of the model area distinguishing the present-day topography. Northwest of Hosskirch along the road towards Tafertsweiler (see Fig. 10), they are separated by geobody E. The complex interfingering of geobody F with geobody E particularly at the northern and southern interfaces is simplified in the 3-D models by an abrupt rise of the boundary layer. Geobody F is commonly 15–25 m thick, but increases up to 40 m towards the western and eastern margins. North–northeast of Hosskirch, the overall thickness decreases to 5–10 m, but is highly variable at short distances. Geobody F is characterised by the occurrence of matrix- to clast-supported diamictons, intercalated fines, diamictic sands, and fine-rich gravels that determine the terminal diamicton association (Dt).

Interpretation Geobody F represents the outline of the terminal moraine that was shaped during the LGM. The steep rise of the Quaternary base towards the north may have hindered any further northward-directed glacier advance during the LGM thus determining the final position of the terminal moraine. The distinct break between the two elongated ridges suggests the existence of a former glacier snout at this particular location. This is furthermore indicated by the regional distribution of proglacial sediments and their palaeoflow directions north of the terminal moraine (see above). Meltwater streams leaving the glacier snout ran parallel to the western ridge and towards Tafertsweiler reworking older sediments and depositing the near-surface, coarse-grained outwash deposits of geobody E.

Geobody G

Description Geobody G caps most parts of geobodies F and E. It reaches a thickness of up to 3 m and commonly consists of weathered deposits of glaciofluvial (Gfw) and glacial (Dw) origin, gravity reworked sediments (GRS) and fluvial deposits (Fl). Weathered deposits of glaciofluvial and glacial origin are associated with the occurrence of gravels and diamictons, respectively, of the underlying geobodies F and E. Gravity reworked sediments mainly occur south of the topographic high in the northwest of the model while fluvial deposits cover a small part in the southwest.

Interpretation Geobody G comprises deposits of Holocene and Late Pleistocene ages. The deposits of this youngest stratigraphic interval in the model region are characterised by postglacial weathering, reworking processes and fluvial activity. These processes influence the raw material potential of exploitable deposits and largely account for non-economic overburden accumulations.

Implications for economic geology

The widespread occurrence of thick coarse-grained glaciofluvial sediments in the study area, specifically the readily accessible near-surface deposits of the last glaciation, designates them as potential exploitation targets. Quaternary gravel and sand deposits are important raw materials and occupy a leading position among the mineral resources in Germany. With an annual production of 43 million tons in the year 2000 (Werner et al. 2002), gravel and sand deposits presently form the key mineral resources in Baden-Württemberg. Gravel and sands are used for road construction and civil engineering, but also constitute supplements in concrete products. Specific grain size classes or materials that require no definite certification are employed in gardening, hydraulic engineering or as filling materials.

The classification of gravel and sand deposits as mineral resources requires a certain quality standard as well as a minimum thickness and extension of the deposit. Genetic origin and stratigraphic age of the raw materials influence material properties in the same way as secondary alteration processes (e.g. weathering, consolidation). As a result, gravel and sand deposits may greatly differ in quantity and quality and not all deposits are suitable for exploitation.

The exposed upper sandy gravel deposits of geobody E (mainly related to the LGM) are typically of a high-quality gravel resource. This is due to their young stratigraphic age and their genetic origin as outwash deposits, which account for an overall lack of matrix-fines. However, their deposition in close proximity to the ice mass caused the formation of diamictic interbeds within the glaciofluvial succession. Subject to the grain size characteristics of the diamictic interlayers (in particular, their amount of fines) as well as their thickness and spatial extension, these horizons are not suitable for exploitation in most cases and have to be removed selectively. The same applies to weathered soil horizons on top of the exploitable deposits (geobody G).

To account for this specific local situation, the quantities of the mineral resources and the residual deposits in the study area were determined on the basis of the 3-D models. Only geobodies E–G were considered which comprise the upper 30–70 m of the Quaternary deposits. The thickness of sandy gravel deposits within the small-scale model generally reaches up to 25 m north of the terminal moraine and consistently increases towards the southeast. This trend is caused by both increasing thickness of outwash deposits linked to the LGM and glaciofluvial deposits associated with the Jungriss stage. The distribution of non-exploitable deposits shows an opposite development. Their thickness increase in the south is primarily caused by diamicton deposits of the terminal moraine and, to a minor degree, by underlying diamicton layers related to the Riss glaciations.

The total thickness of the exploitable deposits in relation to the total thickness of the overburden and intercalated residual horizons largely governs the overall raw material potential of a particular exploration site. Applying the classification of Szenkler and Werner (2000), very high raw material potentials are expected north of the terminal moraine (geobody F) within the sandur deposits of the LGM (Fig. 16). Very high raw material potentials south of the terminal moraine are partly due to thick Jungriss deposits. In contrast to the LGM outwash deposits, quality modifications are expected within these older glaciofluvial sediments. No raw material potential can be attributed to the diamicton deposits of the terminal

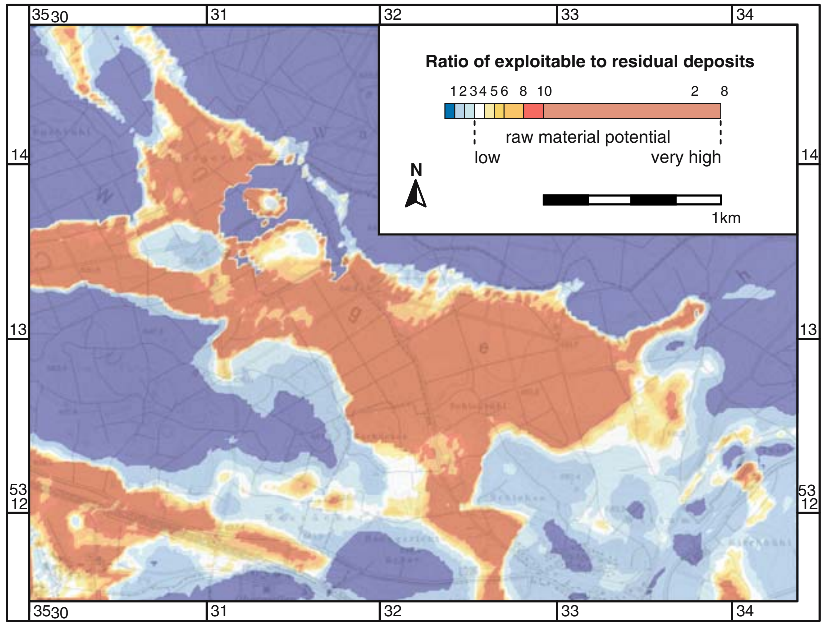

Fig. 16 Map showing the ratio of exploitable to residual deposits within the large-scale model considering the upper 30–70 m of Quaternary deposits. Besides the high quality of the sandy gravel deposits, the raw material potential of the mineral resources is largely determined by the thickness distribution of exploitable deposits in relation to non-exploitable horizons, which define the overall volume of the exploration site

moraine although some thick gravel and sand deposits in the direct vicinity of the terminal moraine (e.g. east of Hosskirch) may locally exhibit a low raw material potential. The lower raw material potential within these deposits is mainly ascribed to a relatively high fraction of non-exploitable interlayers that usually increase exploitation costs.

The designated areas of very high raw material potential (ratio of exploitable to residual deposits greater than 6) approximately cover 305 ha and lead to a total volume of predicted mineral resources of 8.25×10^7 m^3. Based on the representative grain size distribution averaged from data of the two gravel pits, the proportional volume for every grain size class can be determined (Fig. 17). These data provide a measure of the overall quantity of the mineral reservoir potentially available for exploitation in the study area.

Conclusions

- In the present case study, two 3-D geological models of different size and resolution are presented that quantify the distribution of Quaternary deposits in Upper Swabia. The small-scale model focuses on the detailed description of lithofacies associations in the transition zone between the terminal moraine of the LGM and associated sandur covering an area of 2.4 km^2. It is embedded into a larger-scale model that comprises 11.6 km^2.

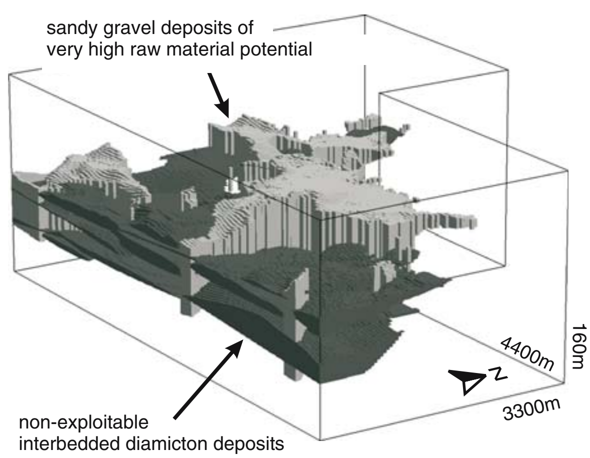

Fig. 17 Modelled volume of exploitable deposits in designated areas of very high raw material potential subdivided into different grain size classes. Volume calculation is based on a representative grain size distribution averaged from data of the two gravel pits

- Both models are characterised by thick glaciofluvial deposits from various glaciations that are interbedded with diamicton deposits of different origin and fine-grained sediments related to interglacial episodes. The interfingering of these diverse deposits reflects the complex history of glacier advances and retreats during several glacial cycles.
- A workflow was developed to derive a hierarchical stratigraphic scheme starting with the analysis of individual lithofacies types in outcrop and core. These form small-scale depositional elements, composing lithofacies associations that are used to derive regional-scale geobodies.
- The spatial distribution of lithofacies associations within large-scale 3-D geobodies was either determined through detailed 3-D mapping or by geostatistical modelling using the variogram-based indicator kriging approach. The models are based on genetic interpretations of core and outcrop data that were integrated with various geophysical surveys in the 3-D modelling program gOcad.
- This paper establishes high-resolution 3-D geological models as a tool to determine the distribution and volume of exploitable mineral deposits. They provide data on economic potential and guide the development of future exploitation targets.

Acknowledgments We want to acknowledge the collaboration with the Landesamt für Geologie, Rohstoffe und Bergbau Baden-Württemberg. In particular, we wish to thank Drs. W. Werner, D. Ellwanger and J. Heinz for their support and helpful discussions. The gravel pit operators Weimar GmbH & Co.KG and Kieswerk Wagenhart GmbH & Co.KG are thanked for giving us permission to access their sites and to use existing core data. This study was funded by the German Research Foundation (grant awarded to G. Teutsch, P. Dietrich and T. Aigner, Te 155/13-1 and Di 833/4-3). The comments of reviewers C. Schlüchter and H. v. Eynatten are gratefully acknowledged.

References

Aber JS, Croot DG, Fenton MM (1989) Glaciotectonic landforms and structures. Kluwer, Dordrecht, pp 1–200

Ashmore PE (1982) Laboratory modelling of gravel braided stream morphology. Earth Surf Proc Land 7:201–225

Becht A (2004) Geophysical methods for the characterization of gravel aquifers: case studies and evaluation experiments. PhD thesis, Tübinger Geowissenschaftliche Arbeiten, C86, University of Tübingen, pp 1–72

Best JL (1988) Sediment transport and bed morphology at river channel confluences. Sedimentology 35:481–498

Best JL, Ashworth PJ (1997) Scour in large braided rivers and the recognition of sequence stratigraphic boundaries. Nature 387:275–277

Bridge JS, Hyndman DW (2004) Aquifer characterization. Society of Economic Paleontologists and Mineralogists Special Publication 80

Bluck BJ (1974) Structure and directional properties of some valley sandur deposits in southern Iceland. Sedimentology 21:533–554

Bluck BJ (1979) Structure of coarse grained braided stream alluvium. Trans Roy Soc Edin-Earth 70:181–221

Boothroyd JC, Ashley GM (1975) Processes, bar morphology, and sedimentary structures on braided outwash fans, northeastern Gulf of Alaska. In: Jopling AV, McDonald BC (eds) Glaciofluvial and glaciolacustrine sedimentation. Society of Economic Paleontologists and Mineralogists (special publication 23), pp 193–222

Bristow C (1996) Reconstructing fluvial channel morphology from sedimentary sequences. In: Carling PA, Dawson MR (eds) Advances in fluvial dynamics and stratigraphy. Wiley, Chichester, pp 351–371

Bristow CS, Best JL, Roy AG (1993) Morphology and facies models of channel confluences. In: Marzo M, Puigdefabregas C (eds) Alluvial Sedimentation. International Association of Sedimentologists (special publication 17), pp 91–100

Brodzikowski K, van Loon AJ (1987) A systematic classification of glacial and periglacial environments, facies and deposits. Earth-Sci Rev 24:297–381

Carling PA (1990) Particle over-passing on depth-limited gravel bars. Sedimentology 37:345–355

Carling PA, Glaister MS (1987) Rapid deposition of sand and gravel mixtures downstream of a negative step: the role of matrix-infilling and particle-overpassing in the process of bar-front accretion. J Geol Soc 144:543–551

Deutsch CV, Journel AG (1992) GSLIB: geostatistical software library and users guide. Oxford University Press, New York, pp 1–340

Ellwanger D, Bibus E, Bludau W, Kösel M, Merkt J, Benda L (1995) Baden-Württemberg. In: Benda L (ed) Das Quartär Deutschlands. Gebrüder Borntraeger, Stuttgart, pp 255–295

Ellwanger D, Bibus E, Bludau W, Fiebig M, Knipping M (1999) Paläoklimatisch-sedimentologische Untersuchungen an Forschungsbohrungen im Quartär des Alpenvorlandes (Rheingletschergebiet/Oberrheingraben). ICDP/KTB-Kolloquium, Wissenschaftliches Programm und Abstracts, Ruhr-University Bochum, pp 77–79

Ellwanger D, Bibus E, Bludau W, Hagedorn E, Storch D (2001) Ansätze zu einer Sequenz- bzw. Klima-Eventstratigraphie der Lockergesteine des südwestdeutschen Alpenvorlandes (Oberschwaben und Oberrhein). ICDP/KTB-Kolloquium, Wissenschaftliches Programm und Abstracts, Ruhr-University of Bochum, pp 43–51

Ellwanger D, Hinderer M, Lämmermann J, Neeb I, Bibus E, Hagedorn E, Villinger E (2002) Sedimentbilanzierungen in quartären und pliozänen Lockergesteinen (Rheingletscher, Mittellandgletscher, Oberrheingraben). ICDP/KTB-Kolloquium, Wissenschaftliches Programm und Abstracts, University of Postdam

Grammer GM, Harris PM, Eberli GP (2004) Integration of outcrop and modern analogs in reservoir modeling. American Association of Petroleum Geologists, Memoir 80

Hambrey MJ (1994) Glacial environments. UCL Press, London, pp 1–296

Harms JC, Southard JB, Walker RG (1982) Structures and sequences in clastic rocks. Society of Economic Paleontologists and Mineralogists, Short Course No 9, pp 1–253

Hein FJ, Walker RG (1977) Bar evolution and development of stratification in the gravelly, braided, Kicking Horse River, British Columbia. Can J Earth Sci 44:562–570

Heinz J (2002) with contributions from Babies HG, Kimmig B, Kostic B, Schuh M, Werner W, Erläuterungen zu Blatt L 8122 Weingarten, Karte der mineralischen Rohstoffe

Baden-Württemberg, 1:50000, Blatt L 8122 Weingarten. Geological Survey of Baden-Württemberg, Freiburg i. Br., pp 1–99
Heinz J, Aigner T (1999) Faziesanalyse und Dynamik würmzeitlicher Sanderablagerungen (Raum Ostrach, Oberschwaben, SW-Deutschland). Zentralblatt für Geol Paläontol 5–6:319–336
Heinz J, Aigner T (2003) Hierarchical dynamic stratigraphy of various Quaternary gravel deposits, Rhine glacier area (SW-Germany): implications for hydrostratigraphy. Int J Earth Sci 92:923–938
Heinz J, Kleineidam S, Teutsch G, Aigner T (2003) Heterogeneity patterns of Quaternary glaciofluvial gravel bodies (SW-Germany): application to hydrogeology. Sediment Geol 158:1–23
Isaaks EH, Srivastava RM (1989) An introduction to applied geostatistics. Oxford University Press, New York, pp 1–561
Keller B (1996) Lithofazies-Codes für die Klassifikation von Lockergesteinen: Mitteilungen der Schweizerischen Gesellschaft für Boden- und Felsmechanik 132:5–12
Lawson DE (1988) Glacigenic resedimentation: classification concepts and application to mass-movement processes and deposits. In: Goldthwait RP, Matsch CL (eds) Genetic classification of glacigenetic deposits. Balkema, Rotterdam, pp 147–169
Levson VM, Rutter NW (1988) A lithofacies analysis and interpretation of depositional environments of montane glacial diamictons, Jasper, Alberta, Canada. In: Goldthwait RP, Matsch CL (eds) Genetic classification of glacigenic deposits. Balkema, Rotterdam, pp 117–140
MacCormack KE, Maclachlan JC, Eyles CH (2005) Viewing the subsurface in three dimensions: initial results of modeling the Quaternary sedimentary infill of the Dundas Valley, Hamilton, Ontario. Geosphere 1:23–31
Marren PM (2001) Sedimentology of proglacial rivers in eastern Scotland during the Late Devensian. Trans Roy Soc Edin Earth-Sci 92:149–171
Nemec W, Steel RJ (1984) Alluvial and coastal conglomerates: their significant features and some comments on gravelly mass-flow deposits. In: Koster EH, Steel RJ (eds) Sedimentology of gravels and conglomerates. Canadian Society of Petroleum Geologists Memoir 10, pp 1–31
Ramos A, Sopena A (1983) Gravel bars in low-sinuosity streams (Permian and Triassic, central Spain). In: Collinson JD, Lewin J (eds) Modern and ancient fluvial systems. International Association of Sedimentologists, (special publication 6), pp 301–312
Rust BR (1978) Depositional models for braided alluvium. In: Miall AD (ed) Fluvial sedimentology. Canadian Society of Petroleum Geologists Memoir 5, pp 605–625
Schreiner A (1992) Einführung in die Quartärgeologie. E. Schweizerbart'sche Verlagsbuchhandlung, Stuttgart, pp 1–257
Siegenthaler C, Huggenberger P (1993) Pleistocene Rhine gravel: deposits of a braided river system with dominant pool preservation. In: Best JL, Bristow CS (eds) Braided Rivers. Geological Society, (special publication 75), pp 147–162
Smith ND (1974) Sedimentology and bar formation in the upper Kicking Horse River, a braided outwash stream. J Geol 82:205–223
Smith SA (1990) The sedimentology and accretionary styles of an ancient gravel-bed stream: the Budleigh Salterton Pebble Beds (Lower Triassic), southwest England. Sediment Geol 67:199–219
Steel RJ, Thompson DB (1983) Structures and textures in Triassic braided stream conglomerates ('Bunter' Pebble Beds) in the Sherwood Sandstone Group, North Staffordshire, England. Sedimentology 30:341–367
Szenkler C, Ellwanger D (2001) Geologische Karte von Baden-Württemberg, 1:25000, Blatt L 8022 Ostrach. Geological Survey of Baden-Württemberg, Freiburg i. Br., 1 sheet
Szenkler C, Werner W (2000) Erläuterungen zu Blatt L 7924/L 7926 Biberach a. d. Riss/ Babenhausen, Karte der mineralischen Rohstoffe Baden-Württemberg, 1:50000. Geological Survey of Baden-Württemberg, Freiburg i. Br., pp 1–156
Todd SP (1989) Stream-driven, high-density gravely traction carpets: possible deposits in the Traberg Conglomerate Formation, SW Ireland and some theoretical considerations of their origin. Sedimentology 36:513–530
Villinger E (2003) Symbolschlüssel Geologie Baden-Württemberg, Geologische Einheiten, Internet Publication www.lgrb.uni-freiburg.de. Geological Survey of Baden-Württemberg, Freiburg i. Br
Wackernagel H (1998) Multivariate statistics, an introduction with applications. Springer, Berlin Heidelberg New York, pp 1–257
Werner W, Kimmig B, Brasse A, Bock W, Finger P, Trapp C, Scholz W, Weinzierl W, Dennert V, Fromm F, Bock H, Köberle G, Kück J, Andrä H (2002) Rohstoffbericht Baden-Württemberg 2002. Geological Survey of Baden-Württemberg, Freiburg i. Br., Informationen 14, pp 1–92
Zielinski T, van Loon AJ (1996) Characteristics and genesis of moraine-derived flowtill varieties. Sediment Geol 101:119–143